Simulating evaporative wet and dry cycles in Gale crater, Mars using thermochemical modeling techniques.

D. Das[1], S.M.R. Turner[2], S.P Schwenzer[2], P. J. Gasda[1], J. Palandri[3], K. Berlo[4], R. J. Leveille[4], L. Crossey[5], B. M. Tutolo[6], N. L. Lanza[1]

[1] Los Alamos National Laboratory, Los Alamos, NM, USA 87545.
[2]AstrobiologyOU, School of Environment, Earth and Ecosystem Sciences, The Open University, Milton Keynes, United Kingdom.
[3]Department of Earth Sciences, University of Oregon, Eugene, USA 97403.
[4]Department of Earth and Planetary Sciences, McGill University, Quebec, Canada H3A 0E8.
[5]Department of Earth and Planetary Sciences, University of New Mexico, NM, USA 87131.
[6]Department of Geoscience, University of Calgary.

Corresponding author: Debarati Das (debaratidas@lanl.gov)

Key points:

- Multiple wet-dry cycles were modeled using thermochemical data for a Gale-relevant scenario to assess the approximate minimum number of cycles to form primary calcium sulfate and borates.
- Based on the results of the model presented in this work, approximately 250 wet-dry cycles (~14, 250 annual cycles on Mars; 25.6 k Earth years) are required to start forming both primary calcium sulfate and borates.
- Primary magnesium sulfates form sooner than calcium sulfate in this model and may explain the presence of magnesium sulfate in Gale crater.

Abstract

The aim of this work is to understand the formation of primary evaporites—sulfates, borates, and chlorides—in Gale crater using thermochemical modeling to determine constraints on their formation. We test the hypothesis that primary evaporites required multiple wet-dry cycles to form, akin to how evaporite assemblages form on Earth. Starting with a basalt-equilibrated Mars fluid, Mars-relevant concentrations of B and Li were added, and then equilibrated with Gale lacustrine bedrock. We simulated cycles of evaporation followed by groundwater recharge/dilution to establish an approximate minimum number of wet-dry cycles required to form primary evaporites. We determine that a minimum of 250 wet-dry cycles may be required to start forming primary evaporites that consist of borates and Ca-sulfates. We estimate that ~14,250 annual cycles (~25.6 k Earth years) of wet and dry periods may form primary borates and Ca-sulfates in Gale crater. These primary evaporites could have been remobilized during secondary diagenesis to form the veins that the Curiosity rover observes in Gale crater. No LiCl salts form after 14,250 cycles modeled for the Gale-relevant scenario (approximately 10^6 cycles would be needed) which implies Li may be leftover in a groundwater brine after the time of the lake. No major deposits of borates are observed to date in Gale crater which also implies that B may be leftover in the subsequent groundwater brine that formed after evaporites were remobilized into Ca-sulfate veins.

Plain Language Summary

Evaporites calcium-sulfate and borates form in dry lakes of Earth due to seasonal wet-dry cycles. The presence of boron-rich calcium sulfate veins in Gale crater point towards the possibility of primary evaporites that may have formed during similar wet-dry cycles. In this work we simulate wet-dry cycles through thermochemically modeling dilution and evaporation in a Gale-relevant scenario (based on observations made in Gale crater) in order to obtain a constraint on the approximate duration required to form primary (unaltered) Ca-sulfate and borates. Based on the results of this work, we find that approximately 250 wet-dry cycles (~14, 250 annual cycles on Mars; 25.6 k Earth years) could have been required to start forming these primary evaporites in Gale crater.

Keywords

Gale crater, Mars aqueous history, thermochemical model, wet-dry cycles.

1 Introduction

The rock record within Gale crater consists of an ancient lacustrine sequence that shows extensive evidence for aqueous activities that are inferred to consist of fluvial and lacustrine sedimentary deposition and ground-water circulation that took place over multiple generations (Gasda et al., 2022; Kronyak et al., 2019; L'Haridon et al., 2020). One of the important markers of aqueous activities in Gale crater are evaporite minerals. These form as a result of fluid evaporation or freezing and their chemical and physical characteristics are representative of their parent fluid compositions and surrounding environment (Bąbel & Schreiber, 2014; Eugster, 1980; Smykatz-Kloss & Roy, 2010). In Gale crater, calcium sulfate, magnesium sulfate, and halite have been observed (Nachon et al., 2014, 2017; N. H. Thomas et al., 2019; Vaniman et al., 2018). The Ca-sulfate found in veins also contains highly water-soluble elements boron and lithium (Das et al., 2020; Gasda et al., 2017). In this work we use thermochemical modeling techniques to understand the enrichment of B and Li in Ca-sulfate veins of Gale crater.

The presence of B in Ca-sulfate veins of Gale crater is hypothesized to be due to remobilization of preexisting primary evaporites such as borates and Ca-sulfates (Das et al., 2020; Gasda et al., 2017; Schwenzer et al., 2016). Clay minerals have been hypothesized to be reservoirs of Li in acidic fluid conditions (Das et al., 2020). In terrestrial settings, borates commonly intergrow with Ca-sulfates as aggregates of extremely fine crystalline borates consisting of micron-sized crystals (as shown in micrographs in (Hunt, 1966) in dry-lake environments that have experienced multiple wet-dry cycles (Lowenstein et al., 1999; Ortí et al., 1998; Swihart et al., 2014). B-rich fluid or mineral inclusions in Ca-sulfates in terrestrial settings are rarely reported (Karmanocky, 2014; Ortí et al., 1998, 2016). Clay minerals in terrestrial dry lake settings are also reported to show presence of B though mineral surface adsorption in relatively high pH aqueous conditions (pH 9-11) (Karahan et al., 2006; Li & Liu, 2020; M. Nellessen et al., 2020; M. A. Nellessen et al., 2023; Rohmah et al., 2020). Lithium is commonly observed as either adsorbed to the surfaces of clay minerals in the same vicinity as Ca-sulfates (Karahan et al., 2006; Li & Liu, 2020; M. Nellessen et al., 2020; M. A. Nellessen et al., 2023; Rohmah et al., 2020; Warren, 2006) or as lithium chloride in solution of dry lake brines (Song et al., 2017; Xiang et al., 2016) in terrestrial

dry lake environments. LiCl is highly hygroscopic in terrestrial atmospheric conditions and forms a self-solution through its property of deliquescence (Gibbard & Scatchard, 1973). Li-rich fluid inclusions associated with Ca-sulfates are also not commonly reported even in Li-rich brine environments (Ericksen et al., 1978; Yu et al., 2022). A review of the literature on emplacement of Li in terrestrial dry lake settings by (Warren, 2016) reports that most lithium salts are highly soluble and tend to stay in solution or can be adsorbed to playa clays.

In this work, evaporites are referred to as either primary or secondary. Primary evaporites commonly form crusts or crystal accumulates on the brine pool floor (Warren, 2000, 2006). Freshly precipitated evaporites that have not undergone any burial, replacement, dehydration, or dissolution are referred to as "primary." With time and processes such as dissolution with new fluids, and re-precipitation, evaporites can experience diagenesis. Evaporites that have undergone any diagenetic processes are referred to as "secondary" (Warren, 2000, 2006). All evaporites so far observed in Gale crater are interpreted to have formed due to secondary diagenetic processes that consisted of multiple generations of remobilization of primary evaporites by groundwater (Gasda et al., 2017; Kronyak et al., 2019; Schwenzer et al., 2016).

(Schwenzer et al., 2016) and (L'Haridon et al., 2020) suggest that the diagenetic evaporites may have formed from local primary evaporates based on the diagenetic evaporite composition and morphology. In this study, we simulate the conditions required to form primary borates and Ca-sulfates using a Gale relevant fluid while reporting the corresponding Li concentration of the modeled fluid. We do not simulate the secondary diagenetic remobilization processes that are inferred to have affected the primary evaporites (e.g., (Schwenzer et al., 2016) or the Li or B adsorption process to clay minerals inferred for Gale crater (Frydenvang et al., 2020; Gasda et al., 2017). Instead, we focus on establishing a minimum time constraint to form borates and Ca-sulfates starting with a Gale relevant fluid. We test the hypothesis that multiple wet and dry cycles consisting of evaporation and sequential precipitation of primary evaporites from Gale lake (Figure 1, stage 4) followed by remobilization caused by dilution of the remnant late water during groundwater recharge (Figure 1, stage 3) is required to form the primary evaporitic assemblage. This process builds up salinity of the lake over time if the lake is a closed basin as is the case for Gale crater. This eventually leads primary evaporite minerals supersaturation in the lake. We use thermochemical modeling to test this hypothesis as a continuation of previous

thermochemical models established for Gale aqueous fluids (Bridges et al., 2015; Schwenzer et al., 2016; Turner et al., 2021). Determining this minimum number of wet and dry cycles and placing it in the context of the broader Gale crater timeline established using sedimentological observations made by the Curiosity rover enables a better understanding of the window of habitability within Gale.

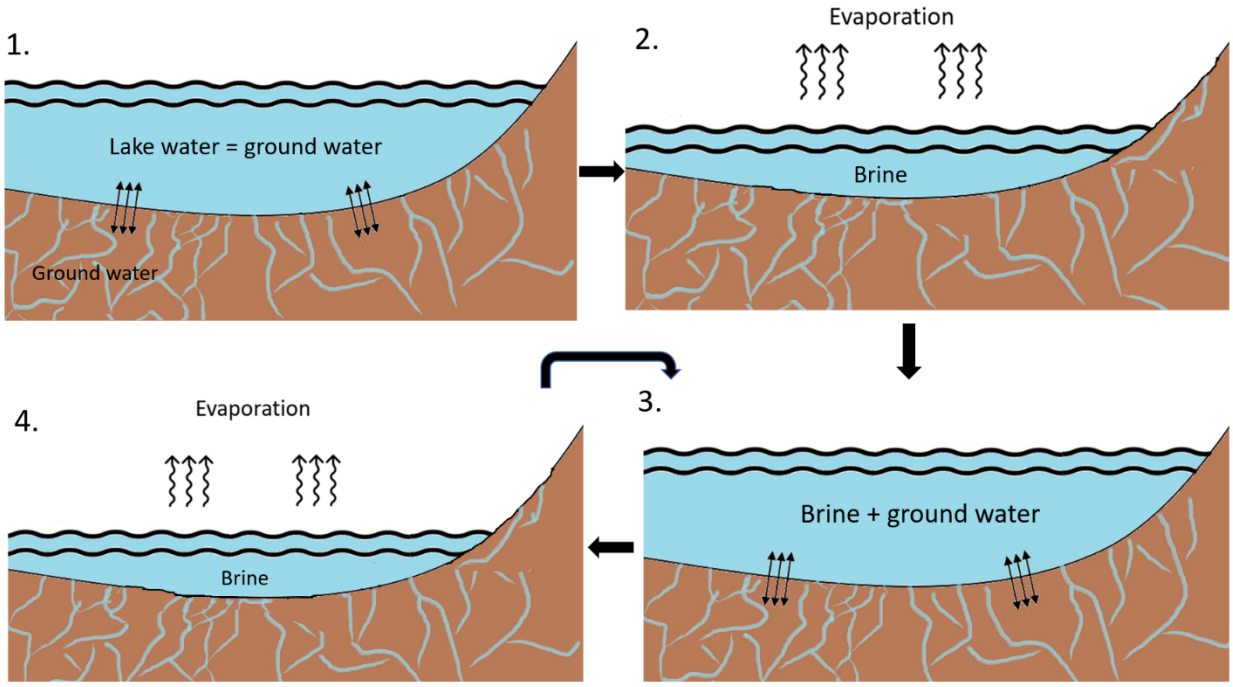

Figure 1. Illustration of the hypothesized sequence of events occurring in Gale crater and tested herein. The sequence involves equilibration of lake water with ground water, cyclic dissolution and evaporation loops. Each component is described in detail in the methodology section.

2 Geologic context of Gale crater

Gale crater is a ~155 km wide crater with a central sedimentary mound (Aeolis Mons, informally known as "Mount Sharp") located between the Southern Highlands and Northern Lowlands division in the northwestern part of the Aeolis quadrangle (Fraeman et al., 2016; Grotzinger & Milliken, 2012; Milliken et al., 2010). The NASA's Mars Science Laboratory (MSL) Curiosity rover landed in Gale crater on Aeolis Palus in 2012 and has since then traversed over 28 km towards Mount Sharp across outcrops interpreted as eolian, fluvial deltaic, and lacustrine deposits (Banham et al., 2018; Edgar et al., 2020; Grotzinger et al., 2014, 2015; Milliken et al., 2010; Stack et al., 2019; Vasavada, 2022; Vasavada et al., 2014).

The geochemistry and sedimentology of rocks in Gale crater points to the presence of an ancient stratified habitable closed basin lake with possible varying lake levels (Grotzinger et al., 2015; Hurowitz et al., 2017) and a long-standing extensive groundwater system (Frydenvang et al., 2017; Gasda et al., 2017, 2022; Siebach & Grotzinger, 2014). The varying lake levels in Gale are inferred from observations of features consistent with lake margin and evaporitic environments (Gwizd et al., 2022; Kah et al., 2018; Stein et al., 2018).

In the lithological unit named the Mount Sharp group in Gale crater, evidence of desiccation and evaporation are observed in the Hartmann's Valley though Sutton Island lithologic members and are interpreted as fluctuating lake margins or a braided river deltaic environment (Fedo et al., 2018; Gwizd et al., 2022; Stein et al., 2018). The evidence includes presence of evaporites (Das et al., 2020; Gasda et al., 2017; N. H. Thomas et al., 2019), desiccation cracks (Stein et al., 2018), altered clay minerals (Bristow et al., 2018), and lithologic facies that are interpreted as lake margin depositional settings (Edgar et al., 2020; Fedo et al., 2018; Gwizd et al., 2022).

In addition to varying lake levels, evidence for multiple stages of aqueous activity throughout much of its history are also observed in Gale crater. The inference of multiple stages of aqueous activity is based on the observation of textures of cross-cutting diagenetic features such as veins. Vein morphology is heterogeneous: they are observed to be massive, nodular, bowl-shaped, boxwork, resistant to erosion, and/or sub-horizontal. Thicker veins display toothy, fibrous, or nodular textures which are interpreted to indicate multiple generations of evaporitic deposition and remobilization within fractures (Das et al., 2020; Gasda et al., 2017; Kronyak et al., 2019, 2019; Nachon et al., 2014, 2017; Schwenzer et al., 2016). Variations in groundwater conditions and ionic species emplaced diagenetic feature chemistry, including veins and nodules, also point to multiple generations of fluids (Comellas et al., 2022; Gasda et al., 2022).

3 Methodology

In this work we used a Gale-relevant fluid and a representative Gale rock composition to simulate cyclic dissolution and evaporation of lake water (details in section 3.1 and 3.2). Prior to executing the simulation steps, we have updated the Holland and Powell (2011) based soltherm thermochemical database of the modeling program used (CHIM-XPT; Reed, 1998) to include

phases that are relevant for this work (i.e., borates) and tested the updated database using a terrestrial analog fluid composition (details in 3.3). Following the database update and testing, we used CHIM-XPT to simulate fluid-rock equilibration, fluid-fluid mixing, and evaporation (details in section 3.4). We simulated four cycles of wet and dry periods using CHIM-XPT and based on the composition of the resultant phases, we then extrapolated brine compositions for up to 250 wet and dry cycles to test the minimum number of cycles required to form Ca-sulfates and borates (details in section 3.4). Following this step, we used time constraints established for terrestrial closed lakes to estimate a minimum time constraint for the number of wet and dry cycles required to form Ca-sulfates and borates for a Gale relevant scenario (details in section 5). All data tables, figures, and plots in this work can be found in a Zenodo data repository (data files: Das, 2023, https://doi.org/10.5281/zenodo.7958213; image files: Das, 2023, https://doi.org/10.5281/zenodo.7958292).

3.1 Thermochemical modeling tool

CHIM-XPT (Reed et al., 2010) is a non-commercial program for computing multicomponent heterogeneous chemical equilibria in aqueous–mineral–gas systems. This code was chosen because it has been specifically developed (and the database adjusted) for Mars-relevant basaltic systems (Reed et al., 2010; Reed & Spycher, 2006) and therefore been used extensively in modeling aqueous activities on Mars (Bridges et al., 2015; Filiberto & Schwenzer, 2013; Melwani Daswani et al., 2016; Schwenzer et al., 2012, 2014, 2016, 2016, 2020; Schwenzer & Kring, 2009; Turner et al., 2021). The modeling calculations take place in steps where each step calculates the minimum Gibbs free energy of the system to attain equilibrium for fluids and their potential precipitates in case of evaporation or fluid-fluid mixing and to attain equilibrium between fluid, precipitates, and dissolved rock in case of fluid-rock rock mixing. The calculations are done based on a database consisting of thermochemical properties of minerals and molecular species using a Debye-Hückel approach (Reed et al., 2010). Step sizes are determined based on the requirement of the calculation and are independent of the amount of water in the system as weight ratios (with a base unit of moles) are used for the calculations. The calculations are based on 1 kg (55.5 mol) of water and the water to rock ratio (W/R) is the ratio of fluid to reacted host rock. Precipitates are not fractionated out of the system unless stated

otherwise. No external gas phases are included or replenished in this model. During the modeling gas phases were allowed to form unless stated otherwise.

3.2 Assumptions and limitations

For this work, we start from the hypothesis that the host of the observed B (i.e., present day) in Ca-sulfate veins is borate minerals and the host of Li is clay minerals. This is based on the observation of B in Ca sulfate veins in Gale (Das et al., 2020; Gasda et al., 2017) and that generally Li is observed in bedrock (Frydenvang et al., 2020).

We start by establishing a relevant fluid composition. First, we take the global Mars relevant fluid that represents the basaltic crust—Gale Portage Water (GPW; (Bish et al., 2013; Bridges et al., 2015; Gellert et al., 2015; Schmidt et al., 2014)—and modify it to incorporate B and Li by adding B and Li in abundances observed in Icelandic stream waters (Section 3.4). This is the best available estimate for a global Mars relevant fluid, and titration between this fluid and a Gale relevant rock composition will equilibrate the fluids with local host rock chemistry and can thus be used to simulate a Gale-relevant groundwater composition (Section 3.4.1). We used the median bedrock composition from the Hartmann's Valley member in Gale crater after removing the observation points that hit diagenetic features (Frydenvang et al., 2020) (Section 3.4.1).

Based on the sedimentological observations, we also assume that the wet-dry cycling process takes place in a relatively low temperature range (25°C) and exclude high-temperature phases such as garnet, amphiboles, pyroxenes and high-temperature mica minerals that are known to form in igneous and metamorphic environments. Besides pyroxene, which is a primary igneous component in the Gale sediments, these other minerals have not been detected in Gale crater (Cousin et al., 2017; Morrison et al., 2018, 2018; Rampe et al., 2020; Thorpe et al., 2022; Treiman et al., 2016). We assume that no high-temperature silica polymorphs form in this system.

To simplify the problem, we assumed a linear increase of aqueous species in the model, i.e., in every groundwater recharge step, the same amount of ground water is brought in, and during the evaporation step, the same amount of water evaporates. We also assume that there is a constant supply of the fluids involved. We note that in real geological systems, the amount of material brought into the crater or water evaporated could vary in time, where less recharge occurs during

arid time periods for example, but this model should provide the average over long time periods. To determine a specific constraint on the number of cycles required to form Ca-sulfates and borates in a Gale-like environment, we have minimized the number of processes that participate in this system to include only water-rock interaction (between established Gale relevant fluid and Gale relevant rock composition), evaporation (that results in the formation of brine) water-water mixing (between established Gale relevant fluid and the modeled brine). We also extrapolate the number of cycles required to form observed evaporites such as Mg sulfate and halite based on the results from this model and assuming a linear increase of salts in the water with time.

The results of this work are a minimum constraint and act as a baseline requirement for the start of formation of Ca-sulfates and represent a part of a geologically complex system (i.e., formation of Ca-sulfates and borates through cyclic dissolution and evaporation). For this modeling, we assume that in a period when Gale crater hosted lakes, the ambient pressure and temperature was 1 bar and temperature is 25°C. We assume that the system is closed to reaction with the Martian atmosphere or fluids other than ground water. GPW was equilibrated with Portage soil 185 mbar CO_2 (0.62×10^{-2} mol CO_2/kg H_2O) (Bridges et al., 2015). We assume that one annual cycle on Mars consists of one dry and wet period and that the relative amount of time for the number of cycles can be constrained based on comparison with terrestrial closed lake systems. We note that long time periods can persist between cycles, or that one stage in a cycle could last many years. But cycles in an early Gale environment may not be shorter than seasonal changes that occur in a year (Lewis & Aharonson, 2014), and thus this work establishes an approximate minimum time constraint.

We also assume that in case of evaporation, the lake does not evaporate to dryness. On Earth, when lakes dry, the water table drops. Some very small amount of surface water does evaporate leaving a thin layer of evaporite at the surface, but the brine that hosts the majority of the aqueous species persists underground. A terrestrial example is Estancia Basin, NM where sulfates form on the surface seasonally, and salty water exists just below the surface during the dry season (Szynkiewicz et al., 2009). Indeed, thicker beds of evaporites grow bottom up in water where that salt has reached saturation in that fluid (e.g., (Warren, 2006), and this type of mechanism is what we model in this paper. Based on terrestrial examples and previous global Mars water budget models, we expect that as the majority of liquid water on Mars will have been

sequestered underground after the water on the surface disappeared (e.g., (Scheller et al., 2021). Hence, we assume that the presence of groundwater prevented Gale crater being fully dry in its early aqueous history. In practice, we stop the model with 10 moles of H_2O remaining (~18% of the original added) at the end of each evaporation step.

3.3 Thermochemical database update and testing

The version of CHIM-XPT thermochemical database utilized in this modeling was based off Holland and Powell (2011) and did not include thermochemical parameters for any borate minerals. The thermochemical database did include LiCl (which can be found in solution in terrestrial dry lake brines), however it did not include thermochemical parameters for Li-carbonates or other Li salts. As Li salts are not commonly formed in terrestrial dry lake settings, for this work we only focus on the formation conditions of primary borates and Ca-sulfates and report the abundance of Li in the modeled fluids.

To model the behavior of boron in a Gale relevant evaporative environment using CHIM-XPT, thermochemical parameters of three borates (kernite, borax, and tincalconite) were added to the existing database before performing the modeling. The database was updated with heat capacity coefficients of kernite, borax, and tincalconite based on the values experimentally determined by (Ruhl, 2008).

The updated database was tested by simulating evaporation using a fluid composition from Searles Lake, in Southern California, as analyzed by (Felmy & Weare, 1986). This area was chosen due to the presence of borates in a dry lake environment and due to the availability of brine composition that is known to form borates in the corresponding dry lake system. This test confirmed that borates formed as products of the updated modeling database if evaporation was simulated. Table 1 indicates the composition of the fluid used for testing the updated database.

Table 1. Fluid composition from Searles Lake (Felmy and Weare, 1986) used for testing the updated CHIM-XPT database.

Ions	**Moles/Kg**
Cl^-	5.41
SO_4^-	0.75
HCO_3^-	1.04
Ca_2^+	0.141

Mg_2^+	0.127 E-05
K^+	1.01
Na^+	7.45
Mn_2^+	0.436 E-07
Li^+	0.46
$B_4O_3(OH)_4^-$	2.60

279

280 **3.4 Establishing a Gale relevant scenario to model an evaporative environment.**

281 Evaporative cycling in Gale crater was modeled by first establishing a Gale-relevant fluid that
282 includes B and Li. This 'modified' Gale Portage Water (mGPW) was then titrated with a Gale
283 relevant rock composition to produce the Gale-relevant fluid. In Section 3.4.1, the details about
284 mGPW and the Gale relevant rock composition is described. In Section S1 (supplementary
285 material), details about titrating mGPW with a Gale relevant host rock to establish a Gale
286 relevant fluid is described. Cyclic evaporation and dilution have been modeled using this Gale
287 relevant fluid and the modeling methodology for evaporation and dilution are described in
288 Section S2 in the supplementary material.

289 **3.4.1 Global Mars relevant fluid: Modified Gale Portage Water.**

290 The starting fluid used for the modeling is Gale Portage Water (Bridges et al., 2015; Schwenzer
291 et al., 2016; Schwenzer & Kring, 2009; Turner et al., 2021). GPW was derived from 'adapted
292 water' [a model fluid derived from a Deccan Trap fluid and adjusted to Mars relevant element
293 ratios (Schwenzer & Kring, 2009)] to represent a global Mars relevant groundwater fluid using
294 data from the Curiosity rover (Bridges et al., 2015). GPW has been used in other Gale-model
295 studies (Schwenzer et al., 2016; Turner et al., 2021). Using an established fluid allows us to
296 compare our results directly with the literature, however GPW does not contain B and Li.

297 Therefore, we modified the composition of GPW to include B and Li. We chose average
298 concentrations of B and Li of Icelandic natural waters were used because Icelandic rocks are
299 fresh basalts and are ideally suited for study as a martian water-rock interaction analog
300 (Ehlmann et al., 2012; Schwenzer et al., 2016; Thorpe et al., 2022) and thus Icelandic natural
301 water compositions provide a geologically realistic abundance ratio of B and Li for a Gale-
302 relevant terrain. The amount of B and Li added to the GPW composition is an average of

Icelandic stream water from Reykjanes from two natural spring water compositions (Spring 1967 and Spring 1918) reported by (Ólafsson & Riley, 1978): 11 ppm B and 8 ppm Li, respectively.

When compared to Icelandic fluids, GPW is lower in abundance of SiO_2, Ca^{2+}, Mg^{2+}, K^+, Na^+, and Mn^{2+} (Table 2). This is due to the extent of weathering in Gale crater based on the observation of minerals such as (clino)pyroxene, and plagioclase in every rock sample of the lacustrine bedrock (Bridges et al., 2015; Rampe et al., 2020) indicating that Ca-containing minerals clinopyroxene and plagioclase were only partially altered (Mangold et al., 2019). The presence of these minerals in the Gale crater bedrock indicates that Gale experienced enough weathering to produce smectite clays from olivine but did not fully weather all the igneous minerals in the sediment (Bridges et al., 2015; Morrison et al., 2018; Thorpe et al., 2022).

The composition of GPW is based on observations made in Gale crater and measurements of martian meteorites and is different from Icelandic fluids, which are derived from a higher extent of aqueous alteration. Hence, we will compare mGPW, GPW, and Nahklites, for which there are B and Li compositions, with the Iceland fluid (Table 2). For soluble species S, B, and Li, the composition is within an order of magnitude of Nahklite (Table 2). The redox in the system is controlled by the resultant speciation of sulfur. B and Li are not major rock forming elements in most igneous minerals and are mobile, i.e., they can diffuse out of minerals due to their small size. These elements will quickly go into solution during aqueous alteration and the higher degree of alteration of Iceland has less influence on their concentration in the fluid. Likewise, these are trace elements and will not form a phase that would deplete their concertation in solution. Therefore, we expect that B and Li in mGPW is a good estimate for B and Li concentration in a basaltic fluid on Mars prior to any adsorption to clays.

Table 2: Fluid composition of Gale Portage Water and modification made using Icelandic natural lakes and groundwater. Composition of fluid are indicated in molar concentration (moles/kg of water or rock).

	Original GPW	Modified GPW	Reykjanes Spring water Olaffson and Riley (1978)	Nakhlite meteorite (Lodders, 1998)
Cl^-	5.76 E-03	5.76 E-03	7.8 E-01	2.25 E-03

SO_4^-	3.97 E-03	3.97 E-03	1.7 E-03	5.41 E-03
HCO_3^-	1.68 E-04	1.68 E-04	-	-
SiO_2	3.49 E-05	3.49 E-05	9.3 E-03	8.9 E-00
Ca^{2+}	1.401 E-05	1.401 E-05	5.9 E-02	2.6 E-00
Mg^{2+}	1.27 E-08	1.27 E-08	2.2 E-03	2.9 E-00
K^+	5.02 E-04	5.02 E-04	5.3 E-02	1.2 E-02
Na^+	9.20 E-03	9.20 E-03	6.1 E-01	7.3 E-02
Mn^{2+}	4.36 E-08	4.36 E-08	6.8 E-05	6.7 E-02
Li^+	-	1.15 E-04	1.15 E-04	4.62 E-04
H_3BO_3	-	8.39 E-04	8.39 E-04	5.76 E-04

To establish a fluid relevant to Gale at the time of the lake, prior to diagenesis, we equilibrate the mGPW groundwater with local Gale bedrock. The results of groundwater equilibration can be found in Section S1. We selected the Hartmann's Valley (HV) region for this work as it shows evidence of dehydration in an environment that is inferred to be that of a lake margin (Gwizd et al., 2018, 2022) and choose the mean bedrock composition of HV, obtained by the ChemCam instrument, that is calculated from a dataset where points with obvious diagenetic materials, soils, and out of focus points, have been removed (Frydenvang et al., 2020). This contrasts with APXS data, which is representative of the bulk chemistry of the rock and includes a Ca sulfate component and other diagenetic materials in the rock. The small spot size (100-500 microns) of ChemCam compared to 4 cm for APXS, enables this type of measurement (Gellert et al., 2013; Maurice et al., 2012; Wiens et al., 2012). For comparison, the mean CaO composition of HV without diagenetic points is 1.6 wt% CaO (Table 3) and the APXS measurements of bulk rock (drill tailings) of Oudam on at the base of HV is 4.03 wt% CaO and 3.54 wt% SO_3 and Marimba just above HV is 5.27 wt% CaO and 6.78 wt% SO_3 (Berger et al., 2020). ChemCam does not have a quantification for SO_3, but the mean composition of HV sums to ~97 wt% (Table 3), indicating that there can be no more than 3 wt% of elements not quantified by ChemCam in Table 3 (e.g., S, P, Cl, H etc.), and we assume based on the clay content of these drill samples that the majority of the missing composition in HV is water (N. H. Thomas et al., 2020). Given the low CaO content in the ChemCam composition we use (Table 2), there cannot be any more

than 2.71 wt% SO_3 in the rock, but that would not account for any CaO in clinopyroxene or plagioclase, which we know from the drill data to make up a large proportion of the rock (Rampe et al., 2020). Therefore, we do not use a S composition from APXS, rather we will estimate it from Nahklites, which is a better representation of the original unaltered bedrock. Although we have a quantification of Li in the bedrock (6.8 ppm; (Frydenvang et al., 2020), we also use the Nahklite value for B and Li for HV rock in the model (Table 3) to represent the composition prior to alteration or addition of evaporites.

Table 3. Average bedrock composition of the Hartmann's Valley target area modified with S, Li, and B concentrations measured in Nakhlite meteorites (Lodders, 1998).

Oxide	**Wt%**
SiO_2	53.6
TiO_2	0.94
Al_2O_3	11.9
FeO_T	18.7
MgO	6.5
CaO	1.6
Na_2O	2.58
K_2O	1.16
MnO	0.05
S	0.02
Li	0.0004
B	0.0005
Sum	97.05

4 Results

We hypothesized that we require multiple wet and dry cycles to form an evaporitic assemblage that consists of Ca-sulfate and borates. In this work we model four sets of wet-dry cycles (cycle 0-3) and extrapolate cycles based on the trends determined using the modeled cycle results. We

identify that it takes a minimum of 250 cycles to start forming primary Ca-sulfates and borates. In order to evaporate an extrapolated fluid that has undergone 250 wet-dry cycles we iteratively reduce the H_2O in the fluid as shown in Figure 2. In this section we summarize the cycling and extrapolation results and comparison of the resultant minerals with a terrestrial analog area in Death Valley, California. The methodology and detailed results for cycling and extrapolation can be found in section S3 and S4 respectively.

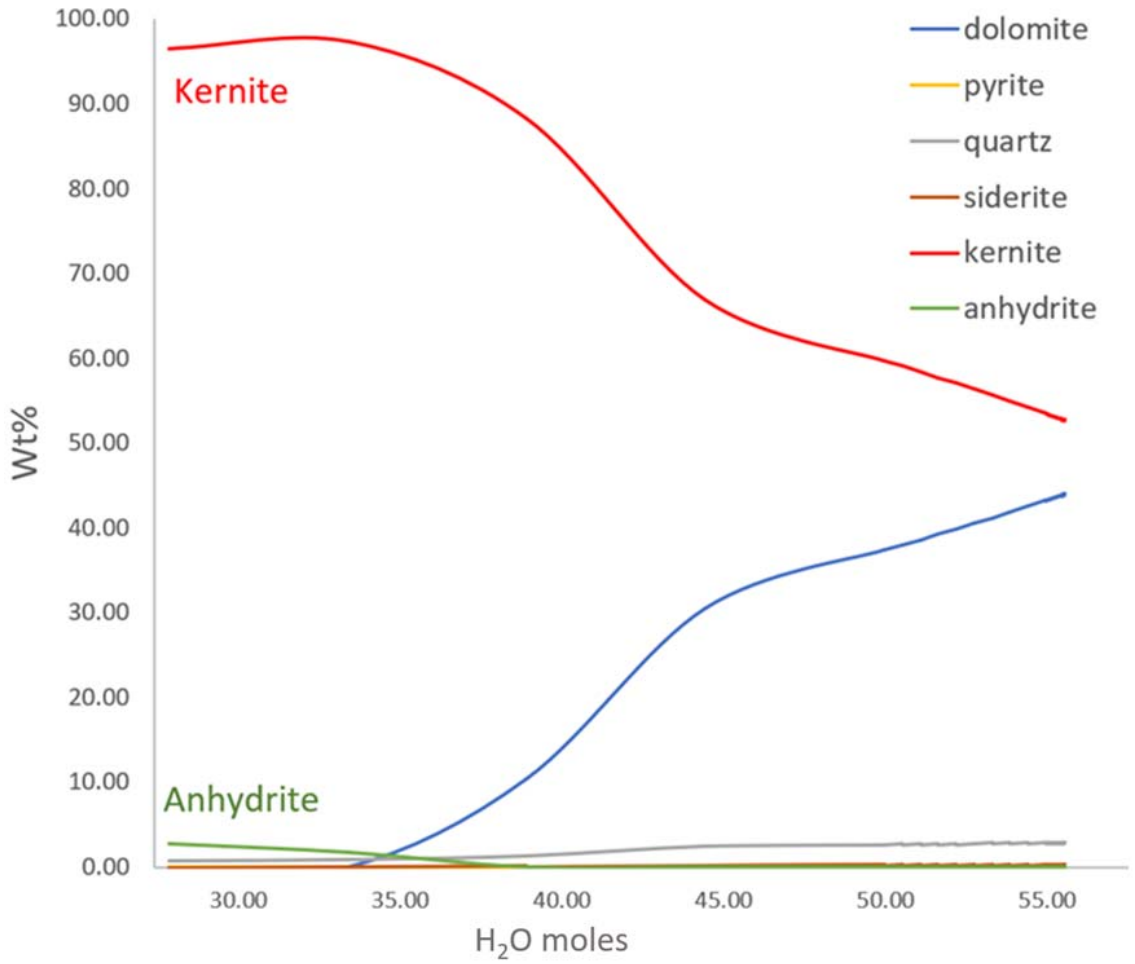

Figure 2. Resultant minerals obtained after evaporating the extrapolated fluid composition that has undergone 250 wet-dry cycles.

Table 4 shows the resultant minerals formed at every modeled and extrapolated dissolution and evaporation stage with corresponding abundance of Li^+ ion in the fluid. The minerals that form in this system are clay minerals (nontronite and kaolinite), evaporites (borates: borax and kernite;

sulfate: anhydrite; carbonates: dolomite, ankerite, dawsonite, siderite), Fe-oxide (hematite, goethite), sulfide (pyrite), chlorites, zeolites, and quartz. Precipitates vary based on the water-rock reaction, evaporation, or fluid-mixing process as shown in Table 4. The extrapolated evaporation stages (cycle 5 to 250) resultant minerals consist of evaporites, sulfides, and quartz. We also note the relative sequence of evaporite formation through the progressive wet-dry cycles and establish that anhydrite (Ca-sulfate) forms in the later stages of the wet-dry cycle compared to borates.

Table 4. Minerals formed throughout the modeled steps (titration, evaporation, and fluid-mixing) with corresponding molar concentration (moles/kg) of Li^+ ions in the fluid:

Cycle	**Process**	**Phases**	**Li^+**
Gale lake fluid	Titration (modeled)	Nontronite, Kaolinite, Hematite, Pyrite, Quartz, Zeolites, Chlorite	9.91E-05
Gale lake evap	Evaporation (modeled)	Quartz, Borax Dolomite, Pyrite, Nontronite, Goethite, Siderite, Ankerite, Dawsonite	1.29E-01
0	Fluid mixing (modeled)	Borax, Quartz, Kaolinite	1.29E-02
0	Evaporation (modeled)	Kernite, Quartz, Kaolinite, Dolomite, Dawsonite, Siderite, Pyrite	1.29E-01
1	Fluid mixing (modeled)	Kaolinite	1.30E-02
1	Evaporation (modeled)	Kernite, Quartz, Kaolinite, Dawsonite, Pyrite	1.30E-01
2	Fluid mixing (modeled)	Kaolinite	1.30E-02
2	Evaporation (modeled)	Kernite, Quartz, Kaolinite, Dawsonite, Pyrite	1.19E-01
3	Fluid mixing (modeled)	Kaolinite	1.31E-02
3	Evaporation (modeled)	Kernite, Quartz, Kaolinite, Pyrite	8.49E-02
5	Evaporation (extrapolated)	Kernite, Quartz, Pyrite	8.67E-02
25	Evaporation (extrapolated)	Kernite, Quartz, Pyrite, Siderite	9.33E-02
50	Evaporation	Kernite, Quartz, Pyrite, Siderite	1.03E-01

	(extrapolated)		
75	Evaporation (extrapolated)	Kernite, Quartz, Pyrite, Siderite	1.13E-01
100	Evaporation (extrapolated)	Kernite, Quartz, Pyrite, Siderite	1.23E-01
125	Evaporation (extrapolated)	Kernite, Quartz, Pyrite, Siderite	1.33E-01
150	Evaporation (extrapolated)	Kernite, Dolomite, Quartz, Pyrite, Siderite	1.43E-01
250	Evaporation (extrapolated)	Kernite, Anhydrite, Dolomite, Quartz, Pyrite, Siderite	1.83E-01

384

385 In order to ground truth and assess the applicability of the modeling results, the resultant
386 minerals have been compared with assemblages observed in a dry lake terrestrial analog, Death
387 Valley, CA (Sarrazin et al., 2005; Baldridge et al., 2004), and with assemblages observed in Gale
388 crater. In the case of the terrestrial analog, all the minerals resulting from the simulated wet-dry
389 cycles, except dawsonite, have been observed in Death Valley. In the case of Gale crater, all the
390 minerals forming in this model have either been observed or are inferred to occur in the crater. A
391 detailed comparison of these phases to terrestrial and Gale crater observations in addition to the
392 number of cycles required to form the phases using the model in this work is provided in Table
393 5.

394 **Table 5.** Comparison of minerals resulting from this work to minerals reported in Death Valley
395 and minerals observed or reported plausible in Gale crater:

Minerals	# of cycles required	Death Valley	Gale crater
Clay:			
Nontronite	Both form at titration, evaporation and fluid mixing (0 cycles required)	Observed (El-Maarry et al., 2015; G. W. Thomas & Coleman, 1964)	Observed (Bristow et al., 2017; He et al., 2022; Rampe et al., 2020)
Kaolinite		Observed (Duke, 2020; Kruse et al., 1993)	Observed (Treiman et al., 2016; Vaniman et al., 2014)
Evaporites:			
Borates			

Borax	1	Observed (Crowley, 1993; Muessig et al., 2019)	Plausible (Das et al., 2020; Gasda et al., 2017)
Kernite	1	Observed (Crowley, 1996)	Plausible (Das et al., 2020; Gasda et al., 2017)
<u>Carbonates</u>			
Dolomite	1	Observed (Corsetti & Grotzinger, 2005; Duke, 2020)	Observed (Sutter et al., 2017)
Ankerite	1	Observed (Bouton, 1984; Petterson et al., 2011)	Observed (Rampe et al., 2022)
Dawsonite	1	Not predominantly reported in Death Valley	Plausible (Bridges et al., 2015; Schwenzer et al., 2016; 2020)
Siderite	25	Observed (Klee et al., 2021; Yang et al., 2005)	Observed (Archer et al., 2020)
<u>Sulfate</u>			
Anhydrite	250	Observed (Crowley, 1993; Knott et al., 2018; Roberts & Spencer, 1998)	Observed (Vaniman et al., 2014, 2018)
Fe-oxides:			
Hematite	Both form at titration and	Observed (Baldridge et al., 2004; Kruse et al., 1993)	Observed (Fraeman et al., 2013; L'Haridon et al., 2020)
Goethite	evaporation 0 cycles required)	Observed (Kruse et al., 1993; Minguez et al., 2012)	Plausible (Bridges et al., 2015; Fraeman et al., 2013)
Sulfide:			
Pyrite	1	Observed (Kaufman et al., 2007)	Observed (McAdam et al., 2014; Morris et al., 2015)
Chlorites	Forms at titration	Observed (Ericksen et al., 1978)	Detected (Borlina et al., 2015; Ehlmann et al., 2012)
Zeolites	Forms at titration	Observed (Ericksen et al., 1988; Kruse et al., 1993)	Plausible (Buz et al., 2017; Schwenzer et al., 2012)
Quartz	Forms at titration and up to 250 cycles	Observed (Crowley, 1996)	Plausible (Frydenvang et al., 2017)

5 Discussion

5.1 Constraining time for simulated wet-dry cycles using terrestrial analogs.

Lakes in terrestrial settings vary in their characteristics based on climatic variations. There are broadly three types of lakes based on the ratio of lake inflow and discharge (Langbein, 1961;

401 Moknatian & Piasecki, 2020; Van der Meeren & Verschuren, 2021): perennial lakes (high water
402 content: water never fully evaporates even in drought periods and the system takes a relatively
403 long time to form evaporites), ephemeral lakes (lower water content compared to perennial lakes
404 with significantly low water levels during water periods enabling evaporite formation faster than
405 in perennial lakes), and dry lakes (predominantly dry with sporadic water content which enables
406 fastest evaporite formation compared to other closed lake systems).

407 The time required to complete a wet-dry cycle in lakes with high water content is longer than a
408 system that has lower water content as the time required to evaporate large amounts of water is
409 higher. In order to form a significant amount of primary evaporites (i.e., more than one thin crust
410 of evaporite on the surface of a dry lakebed), long periods of wet and dry cycles are required,
411 which enables salinity to build up in the lake until evaporites can form. In a closed basin such as
412 Gale crater, this occurs more efficiently than in a lake where there is outflow that can carry the
413 ions away. In terrestrial settings the average wet-dry cycling time (i.e., the amount of time
414 required for a closed lake system to complete a cycle comprising of highest water content in a
415 wet period to lowest water content in a dry period) is approximately 1.5 years for dry lakes with
416 sporadic water presence, 9 years for ephemeral lakes, and 65 years for perennial lakes. Figure 3
417 shows an illustration of relative water amounts varying over time with the average cycling time
418 for dry lakes with sporadic water presence, ephemeral lakes, and perennial lakes (compiled from
419 Langbein, 1961; Moknatian and Piasecki, 2020; Van der Meeren and Verschuren, 2021).

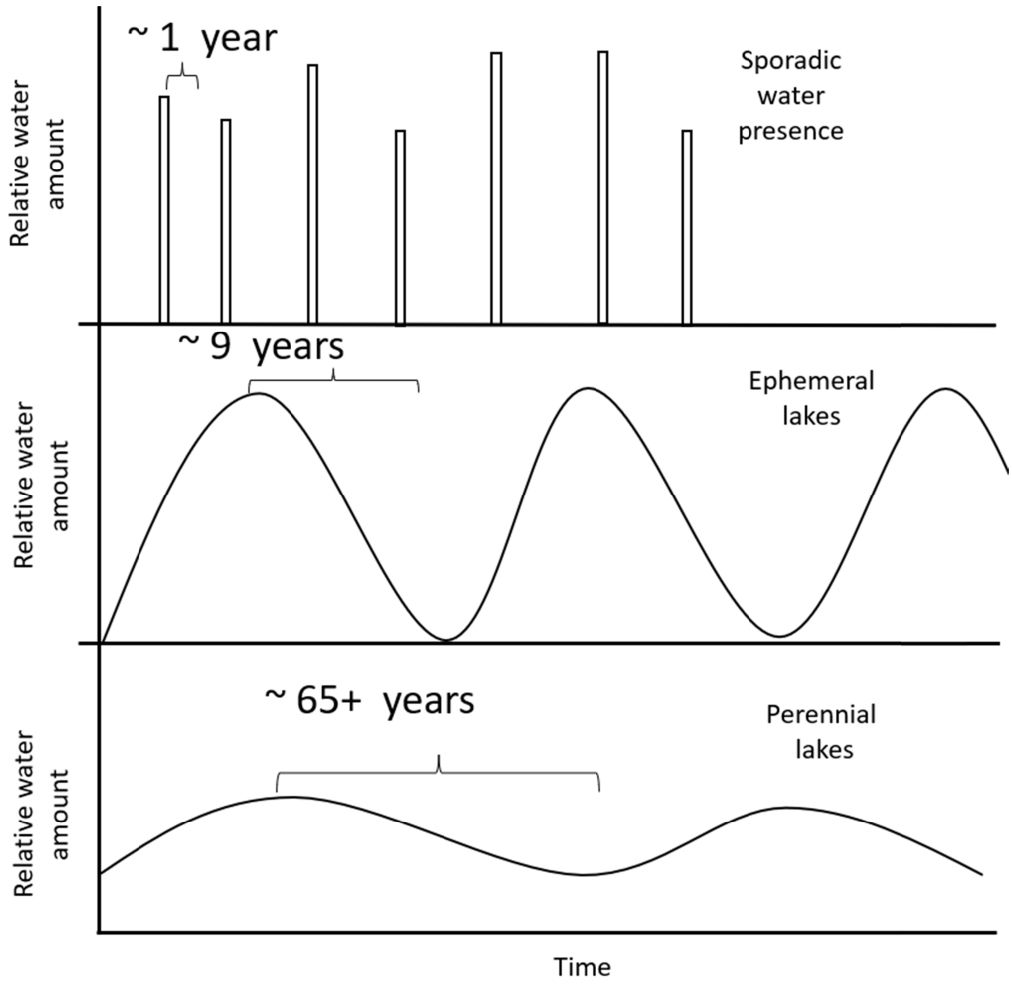

Figure 3. Average wet-dry cycling times for three types of terrestrial closed lakes. The x-axis indicates relative time, and the y-axis indicates relative water amount in the closed lake system (compiled from Langbein, 1961; Moknatian and Piasecki, 2020; Van der Meeren and Verschuren, 2021).

In the following section, we apply the knowledge from terrestrial analogues to estimate relative water levels and lake stages of Gale crater based on the sedimentological observations made by the Curiosity rover and discuss the possible time constraint of wet-dry cycles in Gale crater based on the modeling results and comparison to terrestrial closed lake systems.

5.2 Estimating time constraints for Gale crater primary evaporite formation.

Three lake levels are inferred for Gale crater based on HiRISE (High Resolution Imaging Science Experiment) topographic data collected by the Mars Reconnaissance Orbiter (Palucis et al., 2016). The highest lake level is inferred to have a mean lake depth of 700 m (for the

elevation range -3200 m to -3400 m close to the central mound Mount Sharp area) and is associated with deltaic deposits. The next lake level is inferred to have a mean lake depth of 400 m (for the elevation range -3800 m to -4000 m topographically above the highest elevation sampled by the Curiosity rover to date). The next lake level is inferred to have a mean lake depth of 300 m (for elevation range -4000 m to -4200 m which is the current elevation range the Curiosity rover is measuring) associated with locally sourced water and periods of drying and rewetting. Based on the HiRISE data it is also inferred that Gale experienced a transition from relatively wet regional conditions to drier environments with local runoffs (Palucis et al., 2016).

The mean lake level inferred for the topographic area that has been traversed to date by the Curiosity rover based on HiRISE data is 300 m with intermittent lake level fluctuations (Palucis et al., 2016). The assumption of fluctuating lake levels is also consistent with the inferences made based on observations of sedimentological facies by the Curiosity rover in Gale crater (Hurowitz et al., 2017). The fluctuating lake levels in Gale crater are assumed based on the observations of both fine-grained deposits that indicate relatively deep lake environments (Fedo et al., 2018; Siebach et al., 2019) and the observations of desiccation cracks, altered clay minerals, and presence of higher concentrations of evaporitic elements (e.g., B and Cl) in secondary veins which indicate lake margin with evaporative environments (Bristow et al., 2021; Gasda et al., 2017; Nachon et al., 2017; Stein et al., 2018; N. H. Thomas et al., 2019). The observation by ChemCam that secondary vein chemistry changes with location in the stratigraphy (e.g.,(Gasda et al., 2017, 2022), rather than measuring the same evaporites everywhere in the crater, implies that secondary veins were supplied from the local primary evaporites. The fluctuating lakes levels hypothesis is consistent with the inference that the chemistry and mineralogy of these primary evaporites changed over time in Gale's history. These observations indicate that topography measured to date in Gale crater could have had deep lake levels (up to 300 m) which dropped down to levels that caused the formation of features observed in dry lake environments in terrestrial setting. Based on these observations that are assumed to represent relatively shallow lake levels dropping down to conditions that can form desiccation cracks in the lakebed, we compare possible terrestrial lake types of either ephemeral or lakes with sporadic water presence with Gale crater (consistent with the inferences summarized by (Fedo et al., 2022).

Given these fluctuations in the lake, a number of annual wet-dry cycles can be estimated for Gale crater after a lake type is assigned for the different stratigraphic units based on the sedimentological facies observed in these units (Figure 3). The number of wet-dry cycles are determined by comparing the assigned lake types for Gale crater to common cycling times for terrestrial ephemeral and dry lakes and then the minimum annual wet-dry cycles estimated to form Ca-sulfates and borates from a Gale relevant fluid for this model (Figure 4). We also assume that each stratigraphic unit hosted local primary evaporites that were later remobilized into secondary diagenetic features based on the inferences made by (L'Haridon et al., 2020; Schwenzer et al., 2016)

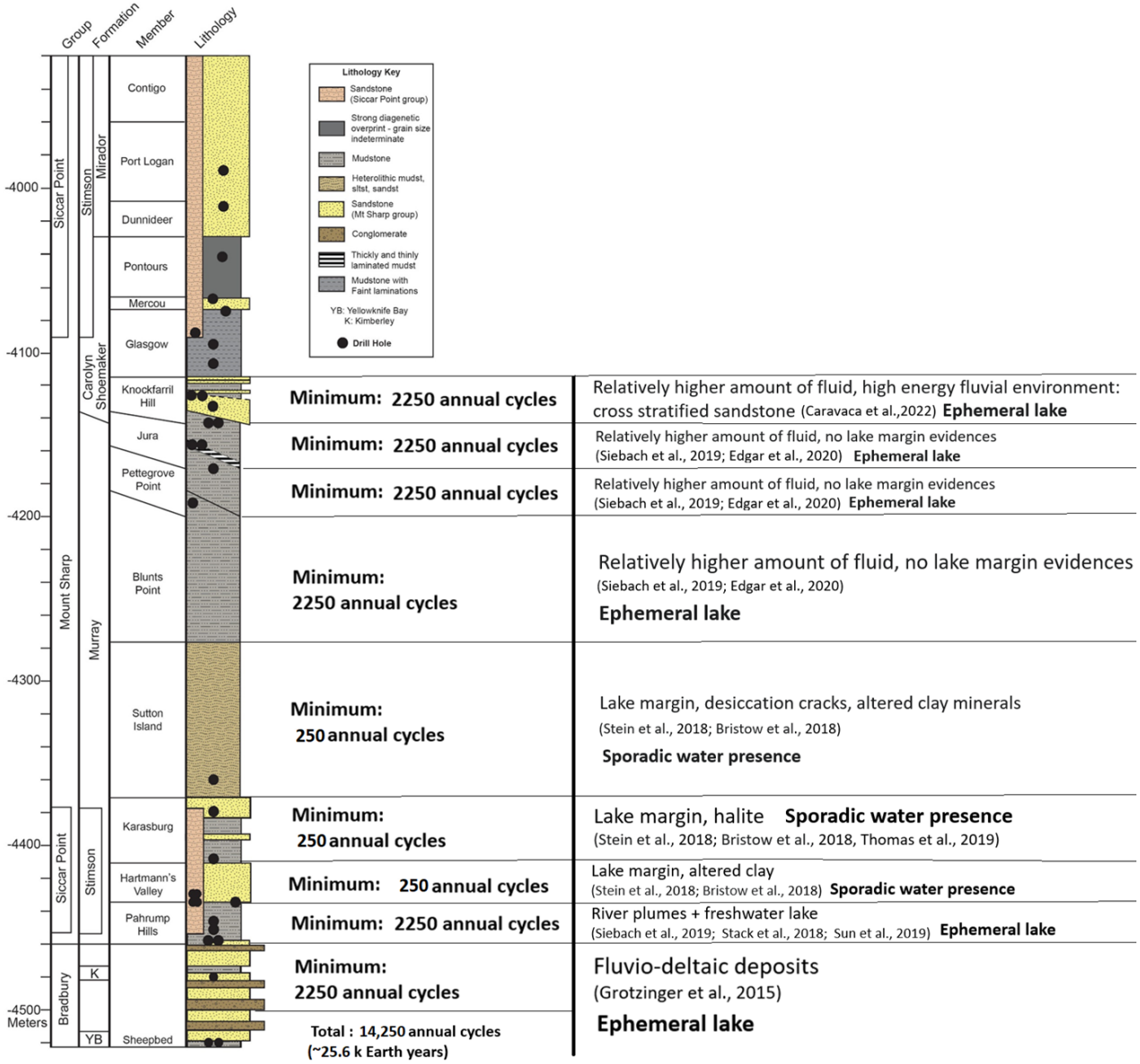

Figure 4. Gale stratigraphic record (Mars Science Laboratory Sedimentology and Stratigraphy Working Group) with minimum annual cycles estimated for forming Ca-sulfates and borates (middle column) based on water levels inferred using observed sedimentological facies (right hand side column).

The Pahrump Hills member is interpreted to represent fluvio-deltaic deposits which is associated with deeper lake levels compared to lake-margin environments (Siebach et al., 2019; Stack et al., 2019; Sun et al., 2019). Hence, we assign an ephemeral lake level for the stratigraphic unit in this elevation range. In terrestrial ephemeral lakes, average amount of time required for one wet-dry

cycle is approximately 9 years (see section 5.1). We estimate that 250 wet-dry cycles in an ephemeral lake would take 2250 (250 times 9) annual cycles on Mars.

Lake-margin environment with episodic lake drying caused by fluctuating lake levels is inferred for the Hartmann's Valley through the Sutton Island members based on the observation of desiccation cracks, altered clay minerals, and the presence of halite (C. Achilles, 2018; Bristow et al., 2018; Fedo et al., 2018; Gwizd et al., 2018; Haber et al., 2019; Siebach et al., 2019, 2019; Stein et al., 2018; N. H. Thomas et al., 2019). Based on the assumption of lake-margin environment for the members Hartmann's Valley, Karasburg, and Sutton Island, we assign the status of sporadic water presence for these members. Based on comparison with cycling times for terrestrial lakes with sporadic water presence (i.e., approximately 1 year), we estimate that 250 wet-dry cycles in a lake with sporadic water presence would take 250 annual cycles on Mars.

The Blunts Point, Pettegrove point, and Jura members show low-energy lacustrine environment based on the presence of fine-grained mudstones which is associated with deeper lake levels compares to lake-margin environments (Caravaca et al., 2022; Edgar et al., 2020; Siebach et al., 2019). We assign ephemeral lake levels for these members and estimate that 250 wet-dry cycles would take 2250 annual cycles per stratigraphic unit.

Based on the relative water levels in Gale estimated using the observed sedimentological facies, the total minimum number of annual cycles required to precipitate sulfates and borates by a Gale relevant fluid using this modeling technique is 14,250. One annual cycle on Mars would include a wet and a dry period and a terrestrial equivalent of this time constraint is approximately 25.6 kyr. This finding is consistent with a wet-dry depositional environment and lake level fluctuations inferred by (Hurowitz et al., 2017). Comparing the minerals predicted to form in our modelling work to observations made in a terrestrial dry lake system and to minerals observed and reported plausible for Gale crater, we find that the minerals in the model are broadly similar to observations made in Death Valley and Gale crater (as shown in Table 4).

5.3 The fate of highly soluble elements in Gale crater brines

While these timescales (Figure 3) seem short, 25.6 kyr is only the time needed to form the first sulfates in the sequence; 10^6 cycles (~10^7 years) are likely needed to accumulate enough Ca to

account for all of the Ca sulfate (e.g., 1% of the volume of the lake sediments, assuming an ephemeral lake) that formed in Gale crater. This value is consistent with timescale of valley and lake formation on Mars (Hoke et al., 2011). After 10^6 cycles, the approximate concentration of B in the fluid (starting with the Gale groundwater composition used in this work) would be 10^5 ppm and the concentration of Li would be 10^4 ppm.

In this model, borates form prior to sulfates. This may likely be due to the uptake of the relatively low amount of the available Ca to form borates earlier in the cycles, while requiring higher number of cycles for the accumulation of enough Ca to form Ca sulfates. The starting fluid (mGPW) contains low amounts of CaO based on the observed extent of weathering in Gale crater (as discussed in Section 3.4.1) and the starting fluid would likely require Ca enrichment over multiple cycles in order to form high Ca-sulfates.

Table S4.2 (in the supplementary material) shows that the concentration of Li^+ ion in the fluid ranges from 9.91E-05 to 1.83E-01 moles/kg (0.7 to 1270 ppm) with 0.7 ppm being the Li^+ concentration of the local Gale lake fluid and 1270 ppm being the Li^+ concentration of the resultant brine after 250 wet-dry cycles. The concentration of Li in the Gale brine is comparable to Li concentration of terrestrial dry lakes that have experienced multiple wet dry seasonal cycles (e.g., an annual average of 1400 ppm in Salar de Atacama and 1062 ppm in Salar de Pastos Grandes: Munk et al., 2016). The saturation point of Li^+ to start forming LiCl at 25°C and 1 bar pressure in 1 kg of water is 1.36×10^5 ppm (Rumble, 2017). Compared to this value, the concentration of Li^+ in the Gale brine of is 10^5 times lower than required to start forming LiCl. However, this concentration is sufficient to form Li-rich clay minerals that form by adsorption of Li on the surface of the clay minerals similar to Li-rich clay minerals observed in terrestrial dry lakes (Warren, 2016; Yu et al., 2022). To start forming LiCl using the starting fluid in this model, approximately 10^6 cycles would be required. We infer that the reservoir of Li in close association with Ca-sulfates of Gale crater are likely clay minerals. However, after 14250 wet dry cycles (as calculated for Gale crater) the Li^+ concentration of the resultant brine would be ~6000 ppm (calculated based on the same extrapolation method described in section S1 in the supplementary material). In Gale crater, the average concentration of Li in veins and sedimentary rocks measured using the Curiosity rover does not exceed ~50 ppm (Das et al., 2020; Frydenvang et al., 2020). Based on the large difference between the observed Li concentration in

Gale crater rocks and Ca-sulfate veins and calculated Li in the remnant brine after simulating wet-dry cycles in a Gale relevant scenario, we infer that Li rich brines may have formed as a remnant subsequent to the lake's disappearance. If this brine was sequestered underground, and no observations of high concentrations of Li deposits have been made, then this remnant brine could still be present underground on Mars.

In Gale crater we also observe the presence of Mg-sulfate (Rapin et al., 2019) and halite (N. H. Thomas et al., 2019). CHIM-XPT is limited by ionic strength of the solution and cannot form phases like Mg-sulfate that are not included in the model. Thus, we use the saturation points of Mg and Na at 1 bar pressure and 25°C for the Gale relevant fluid required to extrapolate the minimum number of wet-dry cycles to form Mg sulfate and halite. We establish that a minimum of 85 cycles are required to form Mg sulfate and a minimum of 200 cycles are required to form halite if there were no competing minerals in the system, for example, Ca-sulfate (competing with Mg-sulfate for the sulfate anion) and nontronite (competing with halite for the Na cation) (Figure 5 and 6). It is likely that Mg-sulfate and halite required a higher number of wet-dry cycles for all the relevant ionic components to saturate because of this competition. Hence the number of wet-dry cycles we have established are a minimum constraint for the number of wet-dry cycles possible in Gale crater and the observation of Mg-sulfate and halite in Gale crater point towards the likelihood of a higher number of wet-dry cycles that Gale crater experienced.

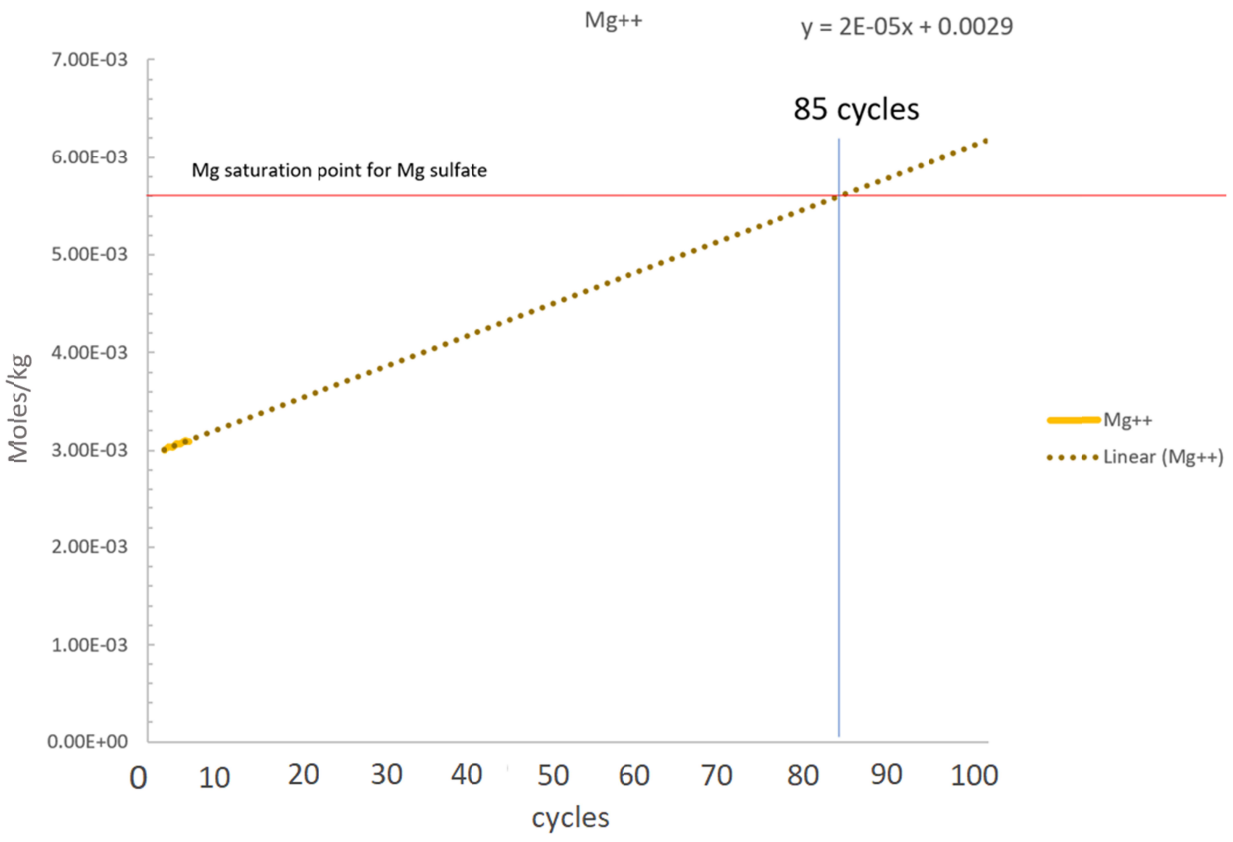

559

560 **Figure 5**. Number of moles/kg of Mg^{2+} for a corresponding amount of SO_4^{2-} to start precipitating
561 Mg-sulfate using the Gale relevant fluid at 1 bar pressure and 25°C.

562

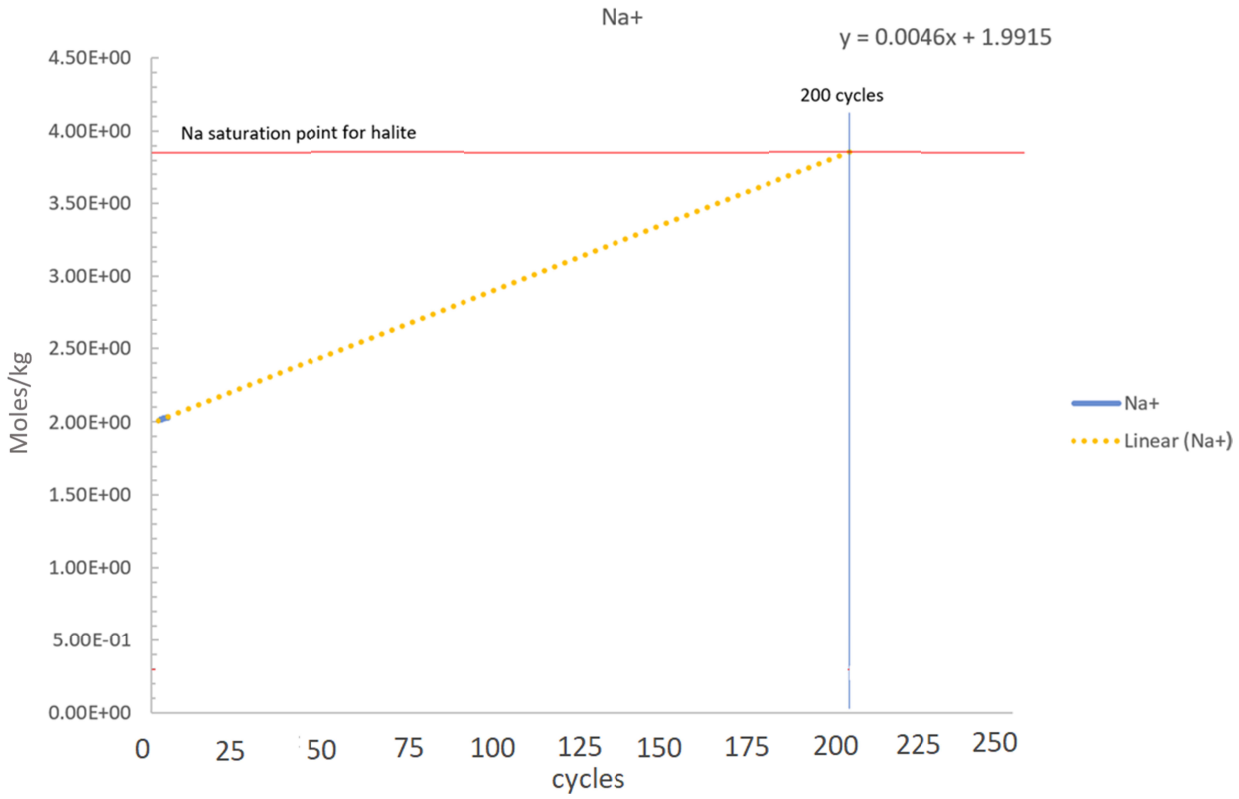

563

564 **Figure 6.** Number of moles/kg of Na^+ for a corresponding amount of Cl^- to start precipitating
565 halite using the Gale relevant fluid at 1 bar pressure and 25°C.

566 **6 Summary and conclusions**

567 In summary, we established that minerals such as clays, quartz and Fe-oxides form in water rock
568 reactions before any evaporation (Table 5). For the formation of formation of primary Ca-
569 sulfates and borates, which are inferred to be precursors of Ca-sulfate veins in Gale crater,
570 multiple wet-dry cycles are required. For the specific Gale-relevant scenario we modeled, a
571 minimum of 250 wet-dry cycles are required to precipitate primary Ca-sulfates, while borate
572 forms immediately. When placed in the larger context of Gale crater's stratigraphy a minimum
573 of ~14000 annual wet dry cycles are required to form primary evaporites consisting of borates
574 and Ca-sulfates with an Li concentration of ~6000 ppm in the resultant brine. Formation of Mg
575 sulfates and halite are also likely in Gale crater at a higher number of cycles than 14000 based on
576 this model.

577 We note that the results of this work add to the assessment of habitability at Gale, as wet-dry
578 cycles have been invoked to be key in the origin of life on Earth (Becker et al., 2019; Hud &

579 Fialho, 2019; Marsh, 2022). Thus, the presence of mineral assemblages in Gale crater that
580 require multiple wet-dry cycles and the estimated duration of over 14k years of those wet-dry
581 cycles, emphasize on the habitability potential during the early stages of Gale crater's aqueous
582 history. Through this work, we present a theoretical geochemical fluid composition and mineral
583 assemblage and duration of the wet-drying cycling environment relevant for Gale crater's early
584 aqueous history which could have resulted in the primary evaporites that are inferred to be
585 precursors of the evaporitic veins observed in Gale crater today.

586 In this work we model fluid and precipitate compositions in wet and dry cycles in Gale crater
587 lakes. The formation of the observed Ca-sulfates and borates in Gale crater require multiple
588 generations of evaporation and dissolution as indeed evidenced by the sedimentary record. The
589 water to rock ratios selected throughout the model are a best estimate based on observations of
590 minerals made using the Curiosity rover. The result of this work shows that a minimum of 250
591 wet dry cycles are required to start forming Ca sulfates and borates from a Gale-relevant fluid at
592 a pressure of 1 bar and at 25°C. Comparing this result to terrestrial closed lake systems and
593 placing the established time constraint in a broader context of Gale's timeline for aqueous
594 activity, a minimum of 14,250 Mars annual cycles (~25.6 k Earth years) is established for the
595 start of formation of primary Ca-sulfates and borates. The result also shows that the
596 concentration of Li in the resultant brine after 250 wet dry cycles is not enough to start forming
597 LiCl, however reaches up to ~6000 ppm after ~14000 wet dry cycles as calculated for Gale
598 crater. Based on the difference between the calculated Li concentration for the leftover brine and
599 observed Li concentration in sedimentary rocks and Ca-sulfates of Gale crater we infer the
600 possibility of underground Li-rich brine that are yet to be encountered.

601 The results of this work are applicable for understanding the evaporative sequence in Gale crater
602 and indicate that in this specific Gale-relevant model, borates form before Ca-sulfates with the
603 formation of Ca-sulfate being the key mineral setting the minimum number of cycles. This work
604 is the first theoretical constraint on fluid composition and mineral assemblages for Gale crater's
605 early aqueous history. Through the results of this work, we estimate the fluid composition and
606 minimum time required to start forming primary evaporites Ca-sulfate and borate (which are
607 inferred to be precursors for Ca-sulfate veins observed in Gale crater today) for the specific
608 Gale-relevant scenario that we chose to model. The results of this work are in accordance with

sedimentological observations that also point towards multiple generations of wet-dry cycles. The results are a lower-limit time estimate for wet-dry cycles and the lifetime of aqueous activity is likely longer when late-stage ground water activity is considered.

7 Conflict of interest

There are no real or perceived financial conflicts of interests for any author. There are also no other affiliations for any author that may be perceived as having a conflict of interest with respect to the results of this paper.

8 Acknowledgements

This work was supported at McGill University, Canada, by the NSERC Discovery program RGPIN-2014-03882, and the Canadian Space Agency's support for Mars Science Laboratory Participating Scientists. Rover data analysis was supported in the United States by the NASA Mars Exploration Program, the Jet Propulsion Laboratory, and Los Alamos National Laboratory. ChemCam operations and science in France was supported by CNRS. Co-authors S.P.S and S.M.R.T acknowledge funding from UK Space Agency Grant ST/S001522/1 and Research England Expanding Excellence in England (E3) fund (Grant code 124.18).

9 Data availability statement

All data and image files supporting the conclusions in this work can be found in Zenodo data repositories (Data sets: Das, 2023, https://doi.org/10.5281/zenodo.7958213 ; Image files: Das, 2023, https://doi.org/10.5281/zenodo.7958292)

References

Achilles, C. (2018). *Analyses of Crystalline and X-Ray Amorphous Materials in Gale Crater Rocks and Soils*. https://repository.arizona.edu/handle/10150/628042

Achilles, C. N., Rampe, E. B., Downs, R. T., Bristow, T. F., Ming, D. W., Morris, R. V., Vaniman, D. T., Blake, D. F., Yen, A. S., McAdam, A. C., Sutter, B., Fedo, C. M., Gwizd, S., Thompson, L. M., Gellert, R., Morrison, S. M., Treiman, A. H., Crisp, J. A., Gabriel, T. S. J., … Morookian, J. M. (2020). Evidence for Multiple Diagenetic Episodes in Ancient Fluvial-Lacustrine Sedimentary Rocks in Gale Crater, Mars. *Journal of*

636 *Geophysical Research: Planets*, *125*(8), e2019JE006295.
637 https://doi.org/10.1029/2019JE006295
638 Archer, P. D., Rampe, E. B., Clark, J. V., Tu, V., Sutter, B., Vaniman, D., Ming, D. W., Franz,
639 H. B., McAdam, A. C., Bristow, T. F., Achilles, C. N., Chipera, S. J., Morrison, S. M.,
640 Thorpe, M. T., Marais, D. J. D., Downs, R. T., Hazen, R. M., Morris, R. V., Treiman, A.
641 H., … Yen, A. S. (2020, March 16). *Detection of Siderite (FeCO3) in Glen Torridon*
642 *Samples by the Mars Science Laboratory Rover*. Lunar and Planetary Science
643 Conference, The Woodlands, TX. https://ntrs.nasa.gov/citations/20200001789
644 Bąbel, M., & Schreiber, B. C. (2014). Geochemistry of Evaporites and Evolution of Seawater. In
645 *Treatise on Geochemistry* (pp. 483–560). Elsevier. https://doi.org/10.1016/B978-0-08-
646 095975-7.00718-X
647 Baldridge, A. M., Farmer, J. D., & Moersch, J. E. (2004). Mars remote-sensing analog studies in
648 the Badwater Basin, Death Valley, California. *Journal of Geophysical Research: Planets*,
649 *109*(E12). https://doi.org/10.1029/2004JE002315
650 Banham, S. G., Gupta, S., Rubin, D. M., Watkins, J. A., Sumner, D. Y., Edgett, K. S.,
651 Grotzinger, J. P., Lewis, K. W., Edgar, L. A., Stack-Morgan, K. M., Barnes, R., Bell III,
652 J. F., Day, M. D., Ewing, R. C., Lapotre, M. G. A., Stein, N. T., Rivera-Hernandez, F., &
653 Vasavada, A. R. (2018). Ancient Martian aeolian processes and palaeomorphology
654 reconstructed from the Stimson formation on the lower slope of Aeolis Mons, Gale
655 crater, Mars. *Sedimentology*, *65*(4), 993–1042. https://doi.org/10.1111/sed.12469
656 Becker, S., Feldmann, J., Wiedemann, S., Okamura, H., Schneider, C., Iwan, K., Crisp, A.,
657 Rossa, M., Amatov, T., & Carell, T. (2019). Unified prebiotically plausible synthesis of
658 pyrimidine and purine RNA ribonucleotides. *Science*, *366*(6461), 76–82.
659 https://doi.org/10.1126/science.aax2747
660 Berger, J. A., Gellert, R., Boyd, N. I., King, P. L., McCraig, M. A., O'Connell-Cooper, C. D.,
661 Schmidt, M. E., Spray, J. G., Thompson, L. M., VanBommel, S. J. V., & Yen, A. S.
662 (2020). Elemental Composition and Chemical Evolution of Geologic Materials in Gale
663 Crater, Mars: APXS Results From Bradbury Landing to the Vera Rubin Ridge. *Journal*
664 *of Geophysical Research: Planets*, *125*(12), e2020JE006536.
665 https://doi.org/10.1029/2020JE006536

666 Bish, D. L., Blake, D. F., Vaniman, D. T., Chipera, S. J., Morris, R. V., Ming, D. W., Treiman,
667 A. H., Sarrazin, P., Morrison, S. M., Downs, R. T., Achilles, C. N., Yen, A. S., Bristow,
668 T. F., Crisp, J. A., Morookian, J. M., Farmer, J. D., Rampe, E. B., Stolper, E. M.,
669 Spanovich, N., … Mier, M.-P. Z. (2013). X-ray Diffraction Results from Mars Science
670 Laboratory: Mineralogy of Rocknest at Gale Crater. *Science*, *341*(6153), 1238932.
671 https://doi.org/10.1126/science.1238932
672 Borlina, C. S., Ehlmann, B. L., & Kite, E. S. (2015). Modeling the thermal and physical
673 evolution of Mount Sharp's sedimentary rocks, Gale Crater, Mars: Implications for
674 diagenesis on the MSL Curiosity rover traverse. *Journal of Geophysical Research:*
675 *Planets*, *120*(8), 1396–1414. https://doi.org/10.1002/2015JE004799
676 Bouton, K. A. (1984). *A spectral reflectance study of the sedimentary paleozoic rocks around*
677 *Racetrack Valley in Death Valley National Monument* [Thesis, California State
678 University, Northridge]. http://dspace.calstate.edu/handle/10211.3/128782
679 Bridges, J. C., Schwenzer, S. P., Leveille, R., Westall, F., Wiens, R. C., Mangold, N., Bristow,
680 T., Edwards, P., & Berger, G. (2015). Diagenesis and clay mineral formation at Gale
681 Crater, Mars. *Journal of Geophysical Research: Planets*, *120*(1), 1–19.
682 https://doi.org/10.1002/2014JE004757
683 Bristow, T. F., Blake, D. F., Vaniman, D. T., Chipera, S. J., Rampe, E. B., Grotzinger, J. P.,
684 McAdam, A. C., Morrison, S. M., Yen, A. S., Morris, R. V., Downs, R. T., Treiman, A.
685 H., Achilles, C. N., & Ma, D. J. D. (2017). *Surveying Clay Mineral Diversity in the*
686 *Murray Formation, Gale Crater, Mars. 38734*.
687 Bristow, T. F., Grotzinger, J. P., Rampe, E. B., Cuadros, J., Chipera, S. J., Downs, G. W., Fedo,
688 C. M., Frydenvang, J., McAdam, A. C., Morris, R. V., Achilles, C. N., Blake, D. F.,
689 Castle, N., Craig, P., Des Marais, D. J., Downs, R. T., Hazen, R. M., Ming, D. W.,
690 Morrison, S. M., … Vasavada, A. R. (2021). Brine-driven destruction of clay minerals in
691 Gale crater, Mars. *Science*, *373*(6551), 198–204. https://doi.org/10.1126/science.abg5449
692 Bristow, T. F., Rampe, E. B., Achilles, C. N., Blake, D. F., Chipera, S. J., Craig, P., Crisp, J. A.,
693 Des Marais, D. J., Downs, R. T., Gellert, R., Grotzinger, J. P., Gupta, S., Hazen, R. M.,
694 Horgan, B., Hogancamp, J. V., Mangold, N., Mahaffy, P. R., McAdam, A. C., Ming, D.
695 W., … Yen, A. S. (2018). Clay mineral diversity and abundance in sedimentary rocks of

696 Gale crater, Mars. *Science Advances*, *4*(6), eaar3330.
697 https://doi.org/10.1126/sciadv.aar3330
698 Buz, J., Ehlmann, B. L., Pan, L., & Grotzinger, J. P. (2017). Mineralogy and stratigraphy of the
699 Gale crater rim, wall, and floor units. *Journal of Geophysical Research: Planets*, *122*(5),
700 1090–1118. https://doi.org/10.1002/2016JE005163
701 Caravaca, G., Mangold, N., Dehouck, E., Schieber, J., Zaugg, L., Bryk, A. B., Fedo, C. M., Le
702 Mouélic, S., Le Deit, L., Banham, S. G., Gupta, S., Cousin, A., Rapin, W., Gasnault, O.,
703 Rivera-Hernández, F., Wiens, R. C., & Lanza, N. L. (2022). From Lake to River:
704 Documenting an Environmental Transition Across the Jura/Knockfarril Hill Members
705 Boundary in the Glen Torridon Region of Gale Crater (Mars). *Journal of Geophysical*
706 *Research: Planets*, *127*(9), e2021JE007093. https://doi.org/10.1029/2021JE007093
707 Comellas, J. M., Essunfeld, A., Morris, R., Lanza, N., Gasda, P. J., Delapp, D., Wiens, R. C.,
708 Gasnault, O., Clegg, S., Bedford, C. C., Dehouck, E., Clark, B. C., Anderson, R., Fisher,
709 W., & Lueth, V. (2022). *Evidence of Multiple Fluid Events in Elevated-Mn ChemCam*
710 *Targets in the Bradbury Rise, Gale Crater, Mars*. *2678*, 2445.
711 Corsetti, F. A., & Grotzinger, J. P. (2005). Origin and Significance of Tube Structures in
712 Neoproterozoic Post-glacial Cap Carbonates: Example from Noonday Dolomite, Death
713 Valley, United States. *PALAIOS*, *20*(4), 348–362. https://doi.org/10.2110/palo.2003.p03-
714 96
715 Cousin, A., Sautter, V., Payré, V., Forni, O., Mangold, N., Gasnault, O., Le Deit, L., Johnson, J.,
716 Maurice, S., Salvatore, M., Wiens, R. C., Gasda, P., & Rapin, W. (2017). Classification
717 of igneous rocks analyzed by ChemCam at Gale crater, Mars. *Icarus*, *288*, 265–283.
718 https://doi.org/10.1016/j.icarus.2017.01.014
719 Crowley, J. K. (1993). Mapping playa evaporite minerals with AVIRIS data: A first report from
720 death valley, California. *Remote Sensing of Environment*, *44*(2), 337–356.
721 https://doi.org/10.1016/0034-4257(93)90025-S
722 Crowley, J. K. (1996). Mg- and K-bearing borates and associated evaporites at Eagle Borax
723 Spring, Death Valley, California; a spectroscopic exploration. *Economic Geology*, *91*(3),
724 622–635. https://doi.org/10.2113/gsecongeo.91.3.622
725 Das, D., Gasda, P. J., Wiens, R. C., Berlo, K., Leveille, R. J., Frydenvang, J., Mangold, N.,
726 Kronyak, R. E., Schwenzer, S. P., Forni, O., Cousin, A., Maurice, S., & Gasnault, O.

(2020). Boron and Lithium in Calcium Sulfate Veins: Tracking Precipitation of Diagenetic Materials in Vera Rubin Ridge, Gale Crater. *Journal of Geophysical Research: Planets*, *125*(8), e2019JE006301. https://doi.org/10.1029/2019JE006301

Das, D. (2023). All data used for thermochemical modeling of wet-dry cycles in Gale crater [data sets]. Zenodo. https://doi.org/10.5281/zenodo.7958213;

Das, D. (2023). All figures for thermochemical modeling of wet-dry cycles in Gale crater [image files], Zenodo. https://doi.org/10.5281/zenodo.7958292).

Duke, E. F. (2020). Mapping metamorphic hydration fronts with field-based near-infrared spectroscopy: Teakettle Junction contact aureole, Death Valley National Park (California, USA). *Geosphere*, *17*(1), 306–321. https://doi.org/10.1130/GES02262.1

Edgar, L. A., Fedo, C. M., Gupta, S., Banham, S. G., Fraeman, A. A., Grotzinger, J. P., Stack, K. M., Stein, N. T., Bennett, K. A., Rivera-Hernández, F., Sun, V. z., Edgett, K. S., Rubin, D. M., House, C., & Van Beek, J. (2020). A Lacustrine Paleoenvironment Recorded at Vera RubinRidge, Gale Crater: Overview of the Sedimentology and Stratigraphy Observed by the Mars ScienceLaboratory Curiosity Rover. *Journal of Geophysical Research: Planets*, *125*(3), e2019JE006307. https://doi.org/10.1029/2019JE006307

Ehlmann, B. L., Bish, D. L., Ruff, S. W., & Mustard, J. F. (2012). Mineralogy and chemistry of altered Icelandic basalts: Application to clay mineral detection and understanding aqueous environments on Mars. *Journal of Geophysical Research: Planets*, *117*(E11). https://doi.org/10.1029/2012JE004156

El-Maarry, M. R., Watters, W. A., Yoldi, Z., Pommerol, A., Fischer, D., Eggenberger, U., & Thomas, N. (2015). Field investigation of dried lakes in western United States as an analogue to desiccation fractures on Mars. *Journal of Geophysical Research: Planets*, *120*(12), 2241–2257. https://doi.org/10.1002/2015JE004895

Ericksen, G. E., Hosterman, J. W., & St. Amand, P. (1988). Chemistry, mineralogy and origin of the clay-hill nitrate deposits, Amargosa River valley, Death Valley region, California, U.S.A. *Chemical Geology*, *67*(1), 85–102. https://doi.org/10.1016/0009-2541(88)90008-3

Ericksen, G. E., Vine, J. D., & Ballón, R. A. (1978). Chemical Composition and Distribution of Lithium-Rich Brines in Salar De Uyuni and Nearby Salars in Southwestern Bolivia. In S.

S. Penner (Ed.), *Lithium Needs and Resources* (pp. 355–363). Pergamon. https://doi.org/10.1016/B978-0-08-022733-7.50020-4

Eugster, H. P. (1980). Geochemistry of Evaporitic Lacustrine Deposits. *Annual Review of Earth and Planetary Sciences*, *8*(1), 35–63. https://doi.org/10.1146/annurev.ea.08.050180.000343

Fedo, C. M., Bryk, A. B., Edgar, L. A., Bennett, K. A., Fox, V. K., Dietrich, W. E., Banham, S. G., Gupta, S., Stack, K. M., Williams, R. M. E., Grotzinger, J. P., Stein, N. T., Rubin, D. M., Caravaca, G., Arvidson, R. E., Hughes, M. N., Fraeman, A. A., Vasavada, A. R., Schieber, J., & Sutter, B. (2022). Geology and Stratigraphic Correlation of the Murray and Carolyn Shoemaker Formations Across the Glen Torridon Region, Gale Crater, Mars. *Journal of Geophysical Research: Planets*, *127*(9), e2022JE007408. https://doi.org/10.1029/2022JE007408

Fedo, C. M., Grotzinger, J. P., Gupta, S., Fraeman, A., Edgar, L., Edgett, K., Stein, N., Rivera-Hernandez, F., Stack, K. M., House, C., Rubin, D., & Vasavada, A. R. (2018). *Sedimentology and Stratigraphy of the Murray Formation, Gale Crater, Mars. 2083*.

Felmy, A. R., & Weare, J. H. (1986). The prediction of borate mineral equilibria in natural waters: Application to Searles Lake, California. *Geochimica et Cosmochimica Acta*, *50*(12), 2771–2783. https://doi.org/10.1016/0016-7037(86)90226-7

Filiberto, J., & Schwenzer, S. P. (2013). Alteration mineralogy of Home Plate and Columbia Hills—Formation conditions in context to impact, volcanism, and fluvial activity. *Meteoritics & Planetary Science*, *48*(10), 1937–1957. https://doi.org/10.1111/maps.12207

Fraeman, A. A., Arvidson, R. E., Catalano, J. G., Grotzinger, J. P., Morris, R. V., Murchie, S. L., Stack, K. M., Humm, D. C., McGovern, J. A., Seelos, F. P., Seelos, K. D., & Viviano, C. E. (2013). A hematite-bearing layer in Gale Crater, Mars: Mapping and implications for past aqueous conditions. *Geology*, *41*(10), 1103–1106. https://doi.org/10.1130/G34613.1

Fraeman, A. A., Edgar, L. A., Rampe, E. B., Thompson, L. M., Frydenvang, J., Fedo, C. M., Catalano, J. G., Dietrich, W. E., Gabriel, T. S. J., Vasavada, A. R., Grotzinger, J. P., L'Haridon, J., Mangold, N., Sun, V. Z., House, C. H., Bryk, A. B., Hardgrove, C., Czarnecki, S., Stack, K. M., … Wong, G. M. (2020). Evidence for a Diagenetic Origin of Vera Rubin Ridge, Gale Crater, Mars: Summary and Synthesis of Curiosity's Exploration

787 Campaign. *Journal of Geophysical Research: Planets*, *125*(12), e2020JE006527.
788 https://doi.org/10.1029/2020JE006527
789 Fraeman, A. A., Ehlmann, B. L., Arvidson, R. E., Edwards, C. S., Grotzinger, J. P., Milliken, R.
790 E., Quinn, D. P., & Rice, M. S. (2016). The stratigraphy and evolution of lower Mount
791 Sharp from spectral, morphological, and thermophysical orbital data sets. *Journal of*
792 *Geophysical Research: Planets*, *121*(9), 1713–1736.
793 https://doi.org/10.1002/2016JE005095
794 Frydenvang, J., Gasda, P. J., Hurowitz, J. A., Grotzinger, J. P., Wiens, R. C., Newsom, H. E.,
795 Edgett, K. S., Watkins, J., Bridges, J. C., Maurice, S., Fisk, M. R., Johnson, J. R., Rapin,
796 W., Stein, N. T., Clegg, S. M., Schwenzer, S. P., Bedford, C. C., Edwards, P., Mangold,
797 N., … Vasavada, A. R. (2017). Diagenetic silica enrichment and late-stage groundwater
798 activity in Gale crater, Mars. *Geophysical Research Letters*, *44*(10), 4716–4724.
799 https://doi.org/10.1002/2017GL073323
800 Frydenvang, J., Mangold, N., Wiens, R. C., Fraeman, A. A., Edgar, L. A., Fedo, C. M.,
801 L'Haridon, J., Bedford, C. C., Gupta, S., Grotzinger, J. P., Bridges, J. C., Clark, B. C.,
802 Rampe, E. B., Gasnault, O., Maurice, S., Gasda, P. J., Lanza, N. L., Olilla, A. M., Meslin,
803 P.-Y., … House, C. H. (2020). The Chemostratigraphy of the Murray Formation and Role
804 of Diagenesis at Vera Rubin Ridge in Gale Crater, Mars, as Observed by the ChemCam
805 Instrument. *Journal of Geophysical Research: Planets*, *125*(9), e2019JE006320.
806 https://doi.org/10.1029/2019JE006320
807 Gasda, P. J., Comellas, J., Essunfeld, A., Das, D., Bryk, A. B., Dehouck, E., Schwenzer, S. P.,
808 Crossey, L., Herkenhoff, K., Johnson, J. R., Newsom, H., Lanza, N. L., Rapin, W.,
809 Goetz, W., Meslin, P.-Y., Bridges, J. C., Anderson, R., David, G., Turner, S. M. R., …
810 Reyes-Newell, A. (2022). Overview of the Morphology and Chemistry of Diagenetic
811 Features in the Clay-Rich Glen Torridon Unit of Gale Crater, Mars. *Journal of*
812 *Geophysical Research: Planets*, *127*(12), e2021JE007097.
813 https://doi.org/10.1029/2021JE007097
814 Gasda, P. J., Haldeman, E. B., Wiens, R. C., Rapin, W., Bristow, T. F., Bridges, J. C.,
815 Schwenzer, S. P., Clark, B., Herkenhoff, K., Frydenvang, J., Lanza, N. L., Maurice, S.,
816 Clegg, S., Delapp, D. M., Sanford, V. L., Bodine, M. R., & McInroy, R. (2017). In situ

detection of boron by ChemCam on Mars. *Geophysical Research Letters*, *44*(17), 8739–8748. https://doi.org/10.1002/2017GL074480

Gellert, R., Berger, J. A., Boyd, N., Brunet, C., Campbell, J. L., Curry, M., Elliott, B., Fulford, P., Grotzinger, J., Hipkin, V., Hurowitz, J. A., King, P. L., Leshin, L. A., Limonadi, D., Pavri, B., Marchand, G., Perrett, G. M., Scodary, A., Simmonds, J. J., … MSL Science Team. (2013). *Initial MSL APXS Activities and Observations at Gale Crater, Mars*. 1432.

Gellert, R., Clark, B. C., III, & MSL and MER Science Teams. (2015). In Situ Compositional Measurements of Rocks and Soils with the Alpha Particle X-ray Spectrometer on NASA's Mars Rovers. *Elements*, *11*(1), 39–44. https://doi.org/10.2113/gselements.11.1.39

Gibbard, H. F., & Scatchard, G. (1973). Liquid-vapor equilibrium of aqueous lithium chloride, from 25 to 100.deg. And from 1.0 to 18.5 molal, and related properties. *Journal of Chemical & Engineering Data*, *18*(3), 293–298. https://doi.org/10.1021/je60058a011

Grotzinger, J. P., Gupta, S., Malin, M. C., Rubin, D. M., Schieber, J., Siebach, K., Sumner, D. Y., Stack, K. M., Vasavada, A. R., Arvidson, R. E., Calef, F., Edgar, L., Fischer, W. F., Grant, J. A., Griffes, J., Kah, L. C., Lamb, M. P., Lewis, K. W., Mangold, N., … Wilson, S. A. (2015). Deposition, exhumation, and paleoclimate of an ancient lake deposit, Gale crater, Mars. *Science*, *350*(6257), aac7575. https://doi.org/10.1126/science.aac7575

Grotzinger, J. P., & Milliken, R. E. (2012). The Sedimentary Rock Record of Mars: Distribution, Origins, and Global Stratigraphy. In J. P. Grotzinger & R. E. Milliken (Eds.), *Sedimentary Geology of Mars* (Vol. 102, p. 0). SEPM Society for Sedimentary Geology. https://doi.org/10.2110/pec.12.102.0001

Grotzinger, J. P., Sumner, D. Y., Kah, L. C., Stack, K., Gupta, S., Edgar, L., Rubin, D., Lewis, K., Schieber, J., Mangold, N., Milliken, R., Conrad, P. G., DesMarais, D., Farmer, J., Siebach, K., Calef, F., Hurowitz, J., McLennan, S. M., Ming, D., … Moores, J. E. (2014). A Habitable Fluvio-Lacustrine Environment at Yellowknife Bay, Gale Crater, Mars. *Science*, *343*(6169), 1242777. https://doi.org/10.1126/science.1242777

Gwizd, S., Fedo, C., Grotzinger, J., Banham, S., Rivera-Hernández, F., Stack, K. M., Siebach, K., Thorpe, M., Thompson, L., O'Connell-Cooper, C., Stein, N., Edgar, L., Gupta, S., Rubin, D., Sumner, D., & Vasavada, A. R. (2022). Sedimentological and Geochemical Perspectives on a Marginal Lake Environment Recorded in the Hartmann's Valley and

Karasburg Members of the Murray Formation, Gale Crater, Mars. *Journal of Geophysical Research: Planets*, *127*(8). https://doi.org/10.1029/2022JE007280

Gwizd, S., Fedo, C., Grotzinger, J., Edgett, K., Rivera-Hernandez, F., & Stein, N. (2018). *Depositional History of the Hartmann's Valley Member, Murray Formation, Gale Crater, Mars*. 2150.

Haber, J. T., Horgan, B., Fraeman, A. A., Johnson, J. R., Wellington, D., Bell, J. F., Starr, M. S., Rice, M. S., & Mangold, N. (2019). *Mineralogy of a Possible Ancient Lakeshore in Gale Crater, Mars, from Mastcam Multispectral Images*. *2089*, 6229.

He, L., Arvidson, R. E., O'Sullivan, J. A., Morris, R. V., Condus, T., Hughes, M. N., & Powell, K. E. (2022). Surface Kinetic Temperatures and Nontronite Single Scattering Albedo Spectra From Mars Reconnaissance Orbiter CRISM Hyperspectral Imaging Data Over Glen Torridon, Gale Crater, Mars. *Journal of Geophysical Research: Planets*, *127*(9), e2021JE007092. https://doi.org/10.1029/2021JE007092

Hoke, M. R. T., Hynek, B. M., & Tucker, G. E. (2011). Formation timescales of large Martian valley networks. *Earth and Planetary Science Letters*, *312*(1), 1–12. https://doi.org/10.1016/j.epsl.2011.09.053

Hud, N. V., & Fialho, D. M. (2019). RNA nucleosides built in one prebiotic pot. *Science*, *366*(6461), 32–33. https://doi.org/10.1126/science.aaz1130

Hunt, C. B. (1966). *Hydrologic Basin, Death Valley, California*. U.S. Government Printing Office.

Hurowitz, J. A., Grotzinger, J. P., Fischer, W. W., McLennan, S. M., Milliken, R. E., Stein, N., Vasavada, A. R., Blake, D. F., Dehouck, E., Eigenbrode, J. L., Fairén, A. G., Frydenvang, J., Gellert, R., Grant, J. A., Gupta, S., Herkenhoff, K. E., Ming, D. W., Rampe, E. B., Schmidt, M. E., … Wiens, R. C. (2017). Redox stratification of an ancient lake in Gale crater, Mars. *Science*, *356*(6341), eaah6849. https://doi.org/10.1126/science.aah6849

Kah, M., Kookana, R. S., Gogos, A., & Bucheli, T. D. (2018). A critical evaluation of nanopesticides and nanofertilizers against their conventional analogues. *Nature Nanotechnology*, *13*(8), Article 8. https://doi.org/10.1038/s41565-018-0131-1

Karahan, S., Yurdakoç, M., Seki, Y., & Yurdakoç, K. (2006). Removal of boron from aqueous solution by clays and modified clays. *Journal of Colloid and Interface Science*, *293*(1), 36–42. https://doi.org/10.1016/j.jcis.2005.06.048

879 Karmanocky, F. (2014). *Fluid inclusion study of gypsum precipitated in acid saline waters:*
880 *Salar Ignorado, northern Chile.*
881 Kaufman, A. J., Corsetti, F. A., & Varni, M. A. (2007). The effect of rising atmospheric oxygen
882 on carbon and sulfur isotope anomalies in the Neoproterozoic Johnnie Formation, Death
883 Valley, USA. *Chemical Geology*, *237*(1), 47–63.
884 https://doi.org/10.1016/j.chemgeo.2006.06.023
885 Klee, J., Chabani, A., Ledésert, B. A., Potel, S., Hébert, R. L., & Trullenque, G. (2021). Fluid-
886 Rock Interactions in a Paleo-Geothermal Reservoir (Noble Hills Granite, California,
887 USA). Part 2: The Influence of Fracturing on Granite Alteration Processes and Fluid
888 Circulation at Low to Moderate Regional Strain. *Geosciences*, *11*(11), Article 11.
889 https://doi.org/10.3390/geosciences11110433
890 Knott, J. R., Machette, M. N., Wan, E., Klinger, R. E., Liddicoat, J. C., Sarna-Wojcicki, A. M.,
891 Fleck, R. J., Deino, A. L., Geissman, J. W., Slate, J. L., Wahl, D. B., Wernicke, B. P.,
892 Wells, S. G., Tinsley, J. C., III, Hathaway, J. C., & Weamer, V. M. (2018). Late
893 Neogene–Quaternary tephrochronology, stratigraphy, and paleoclimate of Death Valley,
894 California, USA. *GSA Bulletin*, *130*(7–8), 1231–1255. https://doi.org/10.1130/B31690.1
895 Kronyak, R. E., Kah, L. C., Edgett, K. S., VanBommel, S. J., Thompson, L. M., Wiens, R. C.,
896 Sun, V. Z., & Nachon, M. (2019). Mineral-Filled Fractures as Indicators of
897 Multigenerational Fluid Flow in the Pahrump Hills Member of the Murray Formation,
898 Gale Crater, Mars. *Earth and Space Science*, *6*(2), 238–265.
899 https://doi.org/10.1029/2018EA000482
900 Kruse, F. A., Lefkoff, A. B., & Dietz, J. B. (1993). Expert system-based mineral mapping in
901 northern death valley, California/Nevada, using the Airborne Visible/Infrared Imaging
902 Spectrometer (AVIRIS). *Remote Sensing of Environment*, *44*(2), 309–336.
903 https://doi.org/10.1016/0034-4257(93)90024-R
904 Langbein, W. B. (1961). *Salinity and Hydrology of Closed Lakes: A Study of the Long-term*
905 *Balance Between Input and Loss of Salts in Closed Lakes*. U.S.GovernmentPrint.Office.
906 Lewis, K. W., & Aharonson, O. (2014). Occurrence and origin of rhythmic sedimentary rocks on
907 Mars. *Journal of Geophysical Research: Planets*, *119*(6), 1432–1457.
908 https://doi.org/10.1002/2013JE004404

L'Haridon, J., Mangold, N., Fraeman, A. A., Johnson, J. R., Cousin, A., Rapin, W., David, G., Dehouck, E., Sun, V., Frydenvang, J., Gasnault, O., Gasda, P., Lanza, N., Forni, O., Meslin, P.-Y., Schwenzer, S. P., Bridges, J., Horgan, B., House, C. H., … Wiens, R. C. (2020). Iron Mobility During Diagenesis at Vera Rubin Ridge, Gale Crater, Mars. *Journal of Geophysical Research: Planets*, *125*(11), e2019JE006299. https://doi.org/10.1029/2019JE006299

Li, W., & Liu, X.-M. (2020). Experimental investigation of lithium isotope fractionation during kaolinite adsorption: Implications for chemical weathering. *Geochimica et Cosmochimica Acta*, *284*, 156–172. https://doi.org/10.1016/j.gca.2020.06.025

Lodders, K. (1998). A survey of shergottite, nakhlite and chassigny meteorites whole-rock compositions. *Meteoritics & Planetary Science*, *33*(S4), A183–A190. https://doi.org/10.1111/j.1945-5100.1998.tb01331.x

Lowenstein, T. K., Li, J., Brown, C., Roberts, S. M., Ku, T.-L., Luo, S., & Yang, W. (1999). 200 k.y. Paleoclimate record from Death Valley salt core. *Geology*, *27*(1), 3–6. https://doi.org/10.1130/0091-7613(1999)027<0003:KYPRFD>2.3.CO;2

Mangold, N., Dehouck, E., Fedo, C., Forni, O., Achilles, C., Bristow, T., Downs, R. T., Frydenvang, J., Gasnault, O., L'Haridon, J., Le Deit, L., Maurice, S., McLennan, S. M., Meslin, P.-Y., Morrison, S., Newsom, H. E., Rampe, E., Rapin, W., Rivera-Hernandez, F., … Wiens, R. C. (2019). Chemical alteration of fine-grained sedimentary rocks at Gale crater. *Icarus*, *321*, 619–631. https://doi.org/10.1016/j.icarus.2018.11.004

Marsh, G. E. (2022). Thermodynamics and the origin of life. *Canadian Journal of Physics*, *100*(6), 285–291. https://doi.org/10.1139/cjp-2020-0013

Maurice, S., Wiens, R. C., Saccoccio, M., Barraclough, B., Gasnault, O., Forni, O., Mangold, N., Baratoux, D., Bender, S., Berger, G., Bernardin, J., Berthé, M., Bridges, N., Blaney, D., Bouyé, M., Caïs, P., Clark, B., Clegg, S., Cousin, A., … Vaniman, D. (2012). The ChemCam Instrument Suite on the Mars Science Laboratory (MSL) Rover: Science Objectives and Mast Unit Description. *Space Science Reviews*, *170*(1), 95–166. https://doi.org/10.1007/s11214-012-9912-2

McAdam, A. C., Franz, H. B., Sutter, B., Archer Jr., P. D., Freissinet, C., Eigenbrode, J. L., Ming, D. W., Atreya, S. K., Bish, D. L., Blake, D. F., Bower, H. E., Brunner, A., Buch, A., Glavin, D. P., Grotzinger, J. P., Mahaffy, P. R., McLennan, S. M., Morris, R. V.,

Navarro-González, R., … Wray, J. J. (2014). Sulfur-bearing phases detected by evolved gas analysis of the Rocknest aeolian deposit, Gale Crater, Mars. *Journal of Geophysical Research: Planets*, *119*(2), 373–393. https://doi.org/10.1002/2013JE004518

McAdam, A. C., Sutter, B., Archer, P. D., Franz, H. B., Wong, G. M., Lewis, J. M. T., Eigenbrode, J. L., Stern, J. C., Knudson, C. A., Clark, J. V., Andrejkovičová, S., Ming, D. W., Morris, R. V., Achilles, C. N., Rampe, E. B., Bristow, T. F., Navarro-González, R., Mahaffy, P. R., Thompson, L. M., … Johnson, S. S. (2020). Constraints on the Mineralogy and Geochemistry of Vera Rubin Ridge, Gale Crater, Mars, From Mars Science Laboratory Sample Analysis at Mars Evolved Gas Analyses. *Journal of Geophysical Research: Planets*, *125*(11), e2019JE006309. https://doi.org/10.1029/2019JE006309

Melwani Daswani, M., Schwenzer, S. P., Reed, M. H., Wright, I. P., & Grady, M. M. (2016). Alteration minerals, fluids, and gases on early Mars: Predictions from 1-D flow geochemical modeling of mineral assemblages in meteorite ALH 84001. *Meteoritics & Planetary Science*, *51*(11), 2154–2174. https://doi.org/10.1111/maps.12713

Milliken, R. E., Grotzinger, J. P., & Thomson, B. J. (2010). Paleoclimate of Mars as captured by the stratigraphic record in Gale Crater. *Geophysical Research Letters*, *37*(4). https://doi.org/10.1029/2009GL041870

Minguez, D. A., Kodama, K. P., & Hillhouse, J. W. (2012). *Magnetic Orbital and Reversal Stratigraphy of the Johnnie Formation, Death Valley region, with implications for the Shuram Carbon Isotope Excursion*. *2012*, GP12A-05.

Moknatian, M., & Piasecki, M. (2020). Lake Volume Data Analyses: A Deep Look into the Shrinking and Expansion Patterns of Lakes Azuei and Enriquillo, Hispaniola. *Hydrology*, *7*(1), Article 1. https://doi.org/10.3390/hydrology7010001

Morris, R. V., Ming, D. W., Gellert, R., Vaniman, D. T., Bish, D. L., Blake, D. F., Chipera, S. J., Morrison, S. M., Downs, R. T., Rampe, E. B., Treiman, A. H., Yen, A. S., Achilles, C. N., Archer, P. D., Bristow, T. F., Cavanaugh, P., Fenrdrich, K., Crisp, J. A., Des Marais, D. J., … Morookian, J. M. (2015, March 16). *Update on the Chemical Composition Of Crystalline, Smectite, and Amorphous Components for Rocknest Soil and John Klein and Cumberland Mudstone Drill Fines at Gale Crater, Mars*. Lunar and Planetary Science Conference, The Woodlands, TX. https://ntrs.nasa.gov/citations/20150001942

971 Morrison, S. M., Downs, R. T., Blake, D. F., Vaniman, D. T., Ming, D. W., Hazen, R. M.,
972 Treiman, A. H., Achilles, C. N., Yen, A. S., Morris, R. V., Rampe, E. B., Bristow, T. F.,
973 Chipera, S. J., Sarrazin, P. C., Gellert, R., Fendrich, K. V., Morookian, J. M., Farmer, J.
974 D., Des Marais, D. J., & Craig, P. I. (2018). Crystal chemistry of martian minerals from
975 Bradbury Landing through Naukluft Plateau, Gale crater, Mars. *American Mineralogist*,
976 *103*(6), 857–871. https://doi.org/10.2138/am-2018-6124
977 Muessig, S. J., Pennell, W. M., Knott, J. R., & Calzia, J. P. (2019). Geology of the Monte Blanco
978 borate deposits, Furnace Creek Wash, Death Valley, California. In *Geology of the Monte*
979 *Blanco borate deposits, Furnace Creek Wash, Death Valley, California* (USGS
980 Numbered Series No. 2019–1111; Open-File Report, Vols. 2019–1111, p. 37). U.S.
981 Geological Survey. https://doi.org/10.3133/ofr20191111
982 Munk, L. A., Hynek, S. A., Bradley, D. C., Boutt, D., Labay, K., & Jochens, H. (2016). Lithium
983 Brines: A Global Perspective. In P. L. Verplanck & M. W. Hitzman (Eds.), *Rare Earth*
984 *and Critical Elements in Ore Deposits* (Vol. 18, p. 0). Society of Economic Geologists.
985 https://doi.org/10.5382/Rev.18.14
986 Nachon, M., Clegg, S. M., Mangold, N., Schröder, S., Kah, L. C., Dromart, G., Ollila, A.,
987 Johnson, J. R., Oehler, D. Z., Bridges, J. C., Le Mouélic, S., Forni, O., Wiens, R. c.,
988 Anderson, R. B., Blaney, D. L., Bell III, J. f., Clark, B., Cousin, A., Dyar, M. D., …
989 Wellington, D. (2014). Calcium sulfate veins characterized by ChemCam/Curiosity at
990 Gale crater, Mars. *Journal of Geophysical Research: Planets*, *119*(9), 1991–2016.
991 https://doi.org/10.1002/2013JE004588
992 Nachon, M., Sumner, D. Y., Borges, S. R., Stack, K., Stein, N., Watkins, J. A., Banham, S.,
993 Rivera-Hernandez, F., Wiens, R. C., l'Haridon, J., Rapin, W., & Kronyak, R. E. (2017).
994 *Stratigraphic distribution of veins in the Murray and Stimson formations, Gale crater,*
995 *Mars: Implications for ancient groundwater circulation*. *2017*, P24B-03.
996 Nellessen, M. A., Gasda, P., Crossey, L., Peterson, E., Ali, A., Zhang, J., Zhou, W., Hao, M.,
997 Spilde, M., Newsom, H., Lanza, N., Reyes-Newell, A., Legett, S., Das, D., Delapp, D.,
998 Yeager, C., Labouriau, A., Clegg, S., & Wiens, R. C. (2023). Boron adsorption in clay
999 minerals: Implications for martian groundwater chemistry and boron on Mars. *Icarus*,
1000 115599. https://doi.org/10.1016/j.icarus.2023.115599

1001 Nellessen, M., Crossey, L., Gasda, P., Newsom, H., Ali, A., Peterson, E., Lanza, N., Reyes-
1002 Newell, A., Delapp, D., Yeager, C., Labouriau, A., Wiens, R., Clegg, S., Legett, S., &
1003 Das, D. (2020). Boron Adsorption In Clay Minerals: Implications for Martian
1004 Groundwater Chemistry And Prebiotic Processes. *Earth and Planetary Sciences ETDs*.
1005 https://digitalrepository.unm.edu/eps_etds/313
1006 Ólafsson, J., & Riley, J. P. (1978). Geochemical studies on the thermal brine from Reykjanes
1007 (Iceland). *Chemical Geology*, *21*(3), 219–237. https://doi.org/10.1016/0009-
1008 2541(78)90046-3
1009 Ortí, F., Helvaci, C., Rosell, L., & Gündoğan, I. (1998). Sulphate–borate relations in an
1010 evaporitic lacustrine environment: The Sultançayir Gypsum (Miocene, western Anatolia).
1011 *Sedimentology*, *45*(4), 697–710. https://doi.org/10.1046/j.1365-3091.1998.00167.x
1012 Ortí, F., Rosell, L., García-Veigas, J., & Helvaci, C. (2016). Sulfate–Borate Association
1013 (Glauberite–Probertite) In the Emet Basin: Implications For Evaporite Sedimentology
1014 (Middle Miocene, Turkey). *Journal of Sedimentary Research*, *86*(5), 448–475.
1015 https://doi.org/10.2110/jsr.2016.32
1016 Palucis, M. C., Dietrich, W. E., Williams, R. M. E., Hayes, A. G., Parker, T., Sumner, D. Y.,
1017 Mangold, N., Lewis, K., & Newsom, H. (2016). Sequence and relative timing of large
1018 lakes in Gale crater (Mars) after the formation of Mount Sharp. *Journal of Geophysical*
1019 *Research: Planets*, *121*(3), 472–496. https://doi.org/10.1002/2015JE004905
1020 Petterson, R., Prave, A. R., Wernicke, B. P., & Fallick, A. E. (2011). The Neoproterozoic
1021 Noonday Formation, Death Valley region, California. *GSA Bulletin*, *123*(7–8), 1317–
1022 1336. https://doi.org/10.1130/B30281.1
1023 Rampe, E. B., Blake, D. F., Bristow, T. F., Ming, D. W., Vaniman, D. T., Morris, R. V.,
1024 Achilles, C. N., Chipera, S. J., Morrison, S. M., Tu, V. M., Yen, A. S., Castle, N., Downs,
1025 G. W., Downs, R. T., Grotzinger, J. P., Hazen, R. M., Treiman, A. H., Peretyazhko, T. S.,
1026 Des Marais, D. J., … Wiens, R. C. (2020). Mineralogy and geochemistry of sedimentary
1027 rocks and eolian sediments in Gale crater, Mars: A review after six Earth years of
1028 exploration with Curiosity. *Geochemistry*, *80*(2), 125605.
1029 https://doi.org/10.1016/j.chemer.2020.125605
1030 Rapin, W., Ehlmann, B. L., Dromart, G., Schieber, J., Thomas, N. H., Fischer, W. W., Fox, V.
1031 K., Stein, N. T., Nachon, M., Clark, B. C., Kah, L. C., Thompson, L., Meyer, H. A.,

Gabriel, T. S. J., Hardgrove, C., Mangold, N., Rivera-Hernandez, F., Wiens, R. C., & Vasavada, A. R. (2019). An interval of high salinity in ancient Gale crater lake on Mars. *Nature Geoscience*, *12*(11), Article 11. https://doi.org/10.1038/s41561-019-0458-8

Reed, M. H. (1998). Calculation of Simultaneous Chemical Equilibria in Aqueous-Mineral-Gas Systems and its Application to Modeling Hydrothermal Processes. In J. P. Richards & P. B. Larson (Eds.), *Techniques in Hydrothermal Ore Deposits Geology* (Vol. 10, p. 0). Society of Economic Geologists. https://doi.org/10.5382/Rev.10.05

Reed, M. H., & Spycher, N. F. (2006). *User's guide for CHILLER: A program for computing water-rock reactions, boiling, mixing and other reaction processes in aqueous-mineralgas systems and minplot guide.* https://scholar.google.com/scholar?hl=en&as_sdt=0%2C32&q=User%E2%80%99s+guide+for+CHILLER%3A+A+program+for+computing+water-rock+reactions%2C+boiling%2C+mixing+and+other+reaction+processes+in+aqueous-mineralgas+systems+and+minplot+guide.&btnG=

Reed, M. H., Spycher, N. F., & Palandri, J. (2010). *User guide for CHIM-XPT: A program for computing reaction processes in aqueous-mineral-gas systems and Minplot guide.*

Roberts, S. M., & Spencer, R. J. (1998). A desert responds to Pleistocene climate change: Saline lacustrine sediments, Death Valley, California, USA. In *Quaternary Deserts and Climatic Change*. CRC Press.

Rohmah, M., Hanum Lalasari, L., Chrisayu Natasha, N., Sulistiyono, E., Firdiyono, F., & Wahyuadi Soedarsono, J. (2020). Adsorption Behavior of Alkali Metal (Na+, Li+, and K+) from Bledug Kuwu brine by Resin Adsorbent for Purification: PH and Flow Rate Parameter. *Oriental Journal of Chemistry*, *36*(02), 273–279. https://doi.org/10.13005/ojc/360209

Ruhl, L. S. (2008). *Thermodynamics of 1: 2 Sodium Borate Minerals.* University of Florida.

Rumble, J. (ed). (2017). *CRC handbook of chemistry and physics*. https://hero.epa.gov/hero/index.cfm/reference/details/reference_id/4731459

Scheller, E. L., Ehlmann, B. L., Hu, R., Adams, D. J., & Yung, Y. L. (2021). Long-term drying of Mars by sequestration of ocean-scale volumes of water in the crust. *Science*, *372*(6537), 56–62. https://doi.org/10.1126/science.abc7717

1062 Schmidt, M. E., Campbell, J. L., Gellert, R., Perrett, G. M., Treiman, A. H., Blaney, D. L., Olilla,
1063 A., Calef III, F. J., Edgar, L., Elliott, B. E., Grotzinger, J., Hurowitz, J., King, P. L.,
1064 Minitti, M. E., Sautter, V., Stack, K., Berger, J. A., Bridges, J. C., Ehlmann, B. L., …
1065 Wiens, R. C. (2014). Geochemical diversity in first rocks examined by the Curiosity
1066 Rover in Gale Crater: Evidence for and significance of an alkali and volatile-rich igneous
1067 source. *Journal of Geophysical Research: Planets*, *119*(1), 64–81.
1068 https://doi.org/10.1002/2013JE004481
1069 Schwenzer, S. P., Abramov, O., Allen, C. C., Bridges, J. C., Clifford, S. M., Filiberto, J., Kring,
1070 D. A., Lasue, J., McGovern, P. J., Newsom, H. E., Treiman, A. H., Vaniman, D. T.,
1071 Wiens, R. C., & Wittmann, A. (2012). Gale Crater: Formation and post-impact hydrous
1072 environments. *Planetary and Space Science*, *70*(1), 84–95.
1073 https://doi.org/10.1016/j.pss.2012.05.014
1074 Schwenzer, S. P., Bridges, J. C., Turner, S. M. R., Ramkissoon, N. K., Cogliati, S., Seidel, R. G.
1075 W., Reed, M. H., Filiberto, J., Vaniman, D., & Olsson-Francis, K. (2020). *Martian Fluids*
1076 *and Their Evaporation Products—An Overview Using Thermochemical Modeling*. 2091.
1077 Schwenzer, S. P., Bridges, J. C., Wiens, R. C., Conrad, P. G., Kelley, S. P., Leveille, R.,
1078 Mangold, N., Martín-Torres, J., McAdam, A., Newsom, H., Zorzano, M. P., Rapin, W.,
1079 Spray, J., Treiman, A. H., Westall, F., Fairén, A. G., & Meslin, P.-Y. (2016). Fluids
1080 during diagenesis and sulfate vein formation in sediments at Gale crater, Mars.
1081 *Meteoritics & Planetary Science*, *51*(11), 2175–2202.
1082 https://doi.org/10.1111/maps.12668
1083 Schwenzer, S. P., Bridges, J., Leveille, R. J., Westall, F., Wiens, R. C., Mangold, N., McAdam,
1084 A., Conrad, P. G., Martín-Torres, J., & Zorzano, M. P. (2014). *Fluids and Sulfate Vein*
1085 *Formation in Gale Crater, Mars. 2014*, P42C-08.
1086 Schwenzer, S. P., & Kring, D. A. (2009). Impact-generated hydrothermal systems capable of
1087 forming phyllosilicates on Noachian Mars. *Geology*, *37*(12), 1091–1094.
1088 https://doi.org/10.1130/G30340A.1
1089 Siebach, K. L., Fedo, C. M., Edgar, L. E., Edgett, K., Grotzinger, J. P., Fraeman, A. A.,
1090 Thompson, L. M., Gupta, S., House, C. H., & O'Connell-Cooper, C. (2019). *Overview of*
1091 *Gale Crater Stratigraphy and Sedimentology from 6 Years of Roving with Mars Science*
1092 *Laboratory*. 1479.

1093 Siebach, K. L., & Grotzinger, J. P. (2014). Volumetric estimates of ancient water on Mount
1094 Sharp based on boxwork deposits, Gale Crater, Mars. *Journal of Geophysical Research:*
1095 *Planets*, *119*(1), 189–198. https://doi.org/10.1002/2013JE004508
1096 Smykatz-Kloss, W., & Roy, P. D. (2010). Evaporite mineralogy and major element geochemistry
1097 as tools for palaeoclimatic investigations in arid regions: A synthesis. *Boletín de La*
1098 *Sociedad Geológica Mexicana*, *62*(3), 379–390.
1099 Song, J. F., Nghiem, L. D., Li, X. M., & He, T. (2017). *Lithium extraction from Chinese salt-lake*
1100 *brines: Opportunities, challenges, and future outlook*.
1101 https://opus.lib.uts.edu.au/handle/10453/125049
1102 Stack, K. M., Grotzinger, J. P., Lamb, M. P., Gupta, S., Rubin, D. M., Kah, L. C., Edgar, L. A.,
1103 Fey, D. M., Hurowitz, J. A., McBride, M., Rivera-Hernández, F., Sumner, D. Y., Van
1104 Beek, J. K., Williams, R. M. E., & Aileen Yingst, R. (2019). Evidence for plunging river
1105 plume deposits in the Pahrump Hills member of the Murray formation, Gale crater, Mars.
1106 *Sedimentology*, *66*(5), 1768–1802. https://doi.org/10.1111/sed.12558
1107 Stein, N., Grotzinger, J. P., Schieber, J., Mangold, N., Hallet, B., Newsom, H., Stack, K. M.,
1108 Berger, J. A., Thompson, L., Siebach, K. L., Cousin, A., Le Mouélic, S., Minitti, M.,
1109 Sumner, D. Y., Fedo, C., House, C. H., Gupta, S., Vasavada, A. R., Gellert, R., …
1110 Dehouck, E. (2018). Desiccation cracks provide evidence of lake drying on Mars, Sutton
1111 Island member, Murray formation, Gale Crater. *Geology*, *46*(6), 515–518.
1112 https://doi.org/10.1130/G40005.1
1113 Sun, V. Z., Stack, K. M., Kah, L. C., Thompson, L., Fischer, W., Williams, A. J., Johnson, S. S.,
1114 Wiens, R. C., Kronyak, R. E., Nachon, M., House, C. H., & VanBommel, S. (2019).
1115 Late-stage diagenetic concretions in the Murray formation, Gale crater, Mars. *Icarus*,
1116 *321*, 866–890. https://doi.org/10.1016/j.icarus.2018.12.030
1117 Sutter, B., McAdam, A. C., Mahaffy, P. R., Ming, D. W., Edgett, K. S., Rampe, E. B.,
1118 Eigenbrode, J. L., Franz, H. B., Freissinet, C., Grotzinger, J. P., Steele, A., House, C. H.,
1119 Archer, P. D., Malespin, C. A., Navarro-González, R., Stern, J. C., Bell, J. F., Calef, F. J.,
1120 Gellert, R., … Yen, A. S. (2017). Evolved gas analyses of sedimentary rocks and eolian
1121 sediment in Gale Crater, Mars: Results of the Curiosity rover's sample analysis at Mars
1122 instrument from Yellowknife Bay to the Namib Dune. *Journal of Geophysical Research:*
1123 *Planets*, *122*(12), 2574–2609. https://doi.org/10.1002/2016JE005225

Swihart, G. H., Carpenter, S. B., Xiao, Y., McBay, E. H., Smith, D. H., & Xiao, Y. (2014). A Boron Isotope Study of the Furnace Creek, California, Borate District. *Economic Geology*, *109*(3), 567–580. https://doi.org/10.2113/econgeo.109.3.567

Szynkiewicz, A., Moore, C. H., Glamoclija, M., & Pratt, L. M. (2009). Sulfur isotope signatures in gypsiferous sediments of the Estancia and Tularosa Basins as indicators of sulfate sources, hydrological processes, and microbial activity. *Geochimica et Cosmochimica Acta*, *73*(20), 6162–6186. https://doi.org/10.1016/j.gca.2009.07.009

Thomas, G. W., & Coleman, N. T. (1964). The Fate of Exchangable Iron in Acid Clay Systems. *Soil Science*, *97*(4), 229.

Thomas, N. H., Ehlmann, B. L., Meslin, P.-Y., Rapin, W., Anderson, D. E., Rivera-Hernández, F., Forni, O., Schröder, S., Cousin, A., Mangold, N., Gellert, R., Gasnault, O., & Wiens, R. C. (2019). Mars Science Laboratory Observations of Chloride Salts in Gale Crater, Mars. *Geophysical Research Letters*, *46*(19), 10754–10763. https://doi.org/10.1029/2019GL082764

Thomas, N. H., Ehlmann, B. L., Rapin, W., Rivera-Hernández, F., Stein, N. T., Frydenvang, J., Gabriel, T., Meslin, P.-Y., Maurice, S., & Wiens, R. C. (2020). Hydrogen Variability in the Murray Formation, Gale Crater, Mars. *Journal of Geophysical Research: Planets*, *125*(9), e2019JE006289. https://doi.org/10.1029/2019JE006289

Thorpe, M. T., Rampe, E. B., Tamborski, J. J., Siebach, K. L., Putnam, A., Kovtun, R., Lynch, K. L., Leeb, D., Gundjonsson, G., Tu, V. M., Ewing, R. C., & Bedford, C. (2022). *Overview and Initial Results of DIGMARS: Digging Iceland Geology for Mars Analog Research Science*. 53rd Lunar and Planetary Science Conference (LPSC), Houston, TX. https://ntrs.nasa.gov/citations/20210026543

Treiman, A. H., Bish, D. L., Vaniman, D. T., Chipera, S. J., Blake, D. F., Ming, D. W., Morris, R. V., Bristow, T. F., Morrison, S. M., Baker, M. B., Rampe, E. B., Downs, R. T., Filiberto, J., Glazner, A. F., Gellert, R., Thompson, L. M., Schmidt, M. E., Le Deit, L., Wiens, R. C., … Yen, A. S. (2016). Mineralogy, provenance, and diagenesis of a potassic basaltic sandstone on Mars: CheMin X-ray diffraction of the Windjana sample (Kimberley area, Gale Crater). *Journal of Geophysical Research: Planets*, *121*(1), 75–106. https://doi.org/10.1002/2015JE004932

Turner, S. M. R., Schwenzer, S. P., Bridges, J. C., Rampe, E. B., Bedford, C. C., Achilles, C. N., McAdam, A. C., Mangold, N., Hicks, L. J., Parnell, J., Fraeman, A. A., & Reed, M. H. (2021). Early diagenesis at and below Vera Rubin ridge, Gale crater, Mars. *Meteoritics & Planetary Science*, *56*(10), 1905–1932. https://doi.org/10.1111/maps.13748

Van der Meeren, T., & Verschuren, D. (2021). Zoobenthos community turnover in a 1650-yr lake-sediment record of climate-driven hydrological change. *Ecosphere*, *12*(1), e03333. https://doi.org/10.1002/ecs2.3333

Vaniman, D. T., Bish, D. L., Ming, D. W., Bristow, T. F., Morris, R. V., Blake, D. F., Chipera, S. J., Morrison, S. M., Treiman, A. H., Rampe, E. B., Rice, M., Achilles, C. N., Grotzinger, J. P., McLennan, S. M., Williams, J., Bell, J. F., Newsom, H. E., Downs, R. T., Maurice, S., … Zorzano Mier, M.-P. (2014). Mineralogy of a Mudstone at Yellowknife Bay, Gale Crater, Mars. *Science*, *343*(6169), 1243480. https://doi.org/10.1126/science.1243480

Vaniman, D. T., Martínez, G. M., Rampe, E. B., Bristow, T. F., Blake, D. F., Yen, A. S., Ming, D. W., Rapin, W., Meslin, P.-Y., Morookian, J. M., Downs, R. T., Chipera, S. J., Morris, R. V., Morrison, S. M., Treiman, A. H., Achilles, C. N., Robertson, K., Grotzinger, J. P., Hazen, R. M., … Sumner, D. Y. (2018). Gypsum, bassanite, and anhydrite at Gale crater, Mars. *American Mineralogist*, *103*(7), 1011–1020. https://doi.org/10.2138/am-2018-6346

Vasavada, A. R. (2022). Mission Overview and Scientific Contributions from the Mars Science Laboratory Curiosity Rover After Eight Years of Surface Operations. *Space Science Reviews*, *218*(3), 14. https://doi.org/10.1007/s11214-022-00882-7

Vasavada, A. R., Grotzinger, J. P., Arvidson, R. E., Calef, F. J., Crisp, J. A., Gupta, S., Hurowitz, J., Mangold, N., Maurice, S., Schmidt, M. E., Wiens, R. C., Williams, R. M. E., & Yingst, R. A. (2014). Overview of the Mars Science Laboratory mission: Bradbury Landing to Yellowknife Bay and beyond. *Journal of Geophysical Research: Planets*, *119*(6), 1134–1161. https://doi.org/10.1002/2014JE004622

Warren, J. K. (2000). Evaporites, brines and base metals: Low-temperature ore emplacement controlled by evaporite diagenesis. *Australian Journal of Earth Sciences*, *47*(2), 179–208. https://doi.org/10.1046/j.1440-0952.2000.00781.x

Warren, J. K. (2006). *Evaporites:Sediments, Resources and Hydrocarbons*. Springer Science & Business Media.

Warren, J. K. (2016). Non-Potash Salts: Borates, Na-Sulphates, Na-Carbonate, Lithium Salts, Gypsum, Halite and Zolites. In J. K. Warren (Ed.), *Evaporites: A Geological Compendium* (pp. 1187–1302). Springer International Publishing. https://doi.org/10.1007/978-3-319-13512-0_12

Wiens, R. C., Maurice, S., Barraclough, B., Saccoccio, M., Barkley, W. C., Bell, J. F., Bender, S., Bernardin, J., Blaney, D., Blank, J., Bouyé, M., Bridges, N., Bultman, N., Caïs, P., Clanton, R. C., Clark, B., Clegg, S., Cousin, A., Cremers, D., … Wong-Swanson, B. (2012). The ChemCam Instrument Suite on the Mars Science Laboratory (MSL) Rover: Body Unit and Combined System Tests. *Space Science Reviews*, *170*(1), 167–227. https://doi.org/10.1007/s11214-012-9902-4

Xiang, W., Liang, S., Zhou, Z., Qin, W., & Fei, W. (2016). Extraction of lithium from salt lake brine containing borate anion and high concentration of magnesium. *Hydrometallurgy*, *166*, 9–15. https://doi.org/10.1016/j.hydromet.2016.08.005

Yang, W., Lowenstein, T. K., Krouse, H. R., Spencer, R. J., & Ku, T.-L. (2005). A 200,000-year δ18O record of closed-basin lacustrine calcite, Death Valley, California. *Chemical Geology*, *216*(1), 99–111. https://doi.org/10.1016/j.chemgeo.2004.11.005

Yu, X., Liu, C., Wang, C., Wang, J., Li, Q., & Meng, L. (2022). Origin of Li brine-type deposits in the Cretaceous gypsum-bearing formation of the Jitai Basin, South China: Constraints from geochemistry and H, O, Li, B, and Sr isotopes. *Applied Geochemistry*, *139*, 105257. https://doi.org/10.1016/j.apgeochem.2022.105257

9 References From the Supporting Information

Achilles, C. N., Rampe, E. B., Downs, R. T., Bristow, T. F., Ming, D. W., Morris, R. V., Vaniman, D. T., Blake, D. F., Yen, A. S., McAdam, A. C., Sutter, B., Fedo, C. M., Gwizd, S., Thompson, L. M., Gellert, R., Morrison, S. M., Treiman, A. H., Crisp, J. A., Gabriel, T. S. J., … Morookian, J. M. (2020). Evidence for Multiple Diagenetic Episodes in Ancient Fluvial-Lacustrine Sedimentary Rocks in Gale Crater, Mars. *Journal of Geophysical Research: Planets*, *125*(8), e2019JE006295. https://doi.org/10.1029/2019JE006295

Fraeman, A. A., Edgar, L. A., Rampe, E. B., Thompson, L. M., Frydenvang, J., Fedo, C. M., Catalano, J. G., Dietrich, W. E., Gabriel, T. S. J., Vasavada, A. R., Grotzinger, J. P., L'Haridon, J., Mangold, N., Sun, V. Z., House, C. H., Bryk, A. B., Hardgrove, C.,

Czarnecki, S., Stack, K. M., … Wong, G. M. (2020). Evidence for a Diagenetic Origin of Vera Rubin Ridge, Gale Crater, Mars: Summary and Synthesis of Curiosity's Exploration Campaign. *Journal of Geophysical Research: Planets*, *125*(12), e2020JE006527. https://doi.org/10.1029/2020JE006527

Langbein, W. B. (1961). *Salinity and Hydrology of Closed Lakes: A Study of the Long-term Balance Between Input and Loss of Salts in Closed Lakes*. U.S.GovernmentPrint.Office.

McAdam, A. C., Sutter, B., Archer, P. D., Franz, H. B., Wong, G. M., Lewis, J. M. T., Eigenbrode, J. L., Stern, J. C., Knudson, C. A., Clark, J. V., Andrejkovičová, S., Ming, D. W., Morris, R. V., Achilles, C. N., Rampe, E. B., Bristow, T. F., Navarro-González, R., Mahaffy, P. R., Thompson, L. M., … Johnson, S. S. (2020). Constraints on the Mineralogy and Geochemistry of Vera Rubin Ridge, Gale Crater, Mars, From Mars Science Laboratory Sample Analysis at Mars Evolved Gas Analyses. *Journal of Geophysical Research: Planets*, *125*(11), e2019JE006309. https://doi.org/10.1029/2019JE006309

Rampe, E. B., Blake, D. F., Bristow, T. F., Ming, D. W., Vaniman, D. T., Morris, R. V., Achilles, C. N., Chipera, S. J., Morrison, S. M., Tu, V. M., Yen, A. S., Castle, N., Downs, G. W., Downs, R. T., Grotzinger, J. P., Hazen, R. M., Treiman, A. H., Peretyazhko, T. S., Des Marais, D. J., … Wiens, R. C. (2020). Mineralogy and geochemistry of sedimentary rocks and eolian sediments in Gale crater, Mars: A review after six Earth years of exploration with Curiosity. *Geochemistry*, *80*(2), 125605. https://doi.org/10.1016/j.chemer.2020.125605

Rapin, W., Ehlmann, B. L., Dromart, G., Schieber, J., Thomas, N. H., Fischer, W. W., Fox, V. K., Stein, N. T., Nachon, M., Clark, B. C., Kah, L. C., Thompson, L., Meyer, H. A., Gabriel, T. S. J., Hardgrove, C., Mangold, N., Rivera-Hernandez, F., Wiens, R. C., & Vasavada, A. R. (2019). An interval of high salinity in ancient Gale crater lake on Mars. *Nature Geoscience*, *12*(11), Article 11. https://doi.org/10.1038/s41561-019-0458-8

Treiman, A. H., Bish, D. L., Vaniman, D. T., Chipera, S. J., Blake, D. F., Ming, D. W., Morris, R. V., Bristow, T. F., Morrison, S. M., Baker, M. B., Rampe, E. B., Downs, R. T., Filiberto, J., Glazner, A. F., Gellert, R., Thompson, L. M., Schmidt, M. E., Le Deit, L., Wiens, R. C., … Yen, A. S. (2016). Mineralogy, provenance, and diagenesis of a potassic basaltic sandstone on Mars: CheMin X-ray diffraction of the Windjana sample

(Kimberley area, Gale Crater). *Journal of Geophysical Research: Planets*, *121*(1), 75–106. https://doi.org/10.1002/2015JE004932

Vaniman, D. T., Martínez, G. M., Rampe, E. B., Bristow, T. F., Blake, D. F., Yen, A. S., Ming, D. W., Rapin, W., Meslin, P.-Y., Morookian, J. M., Downs, R. T., Chipera, S. J., Morris, R. V., Morrison, S. M., Treiman, A. H., Achilles, C. N., Robertson, K., Grotzinger, J. P., Hazen, R. M., … Sumner, D. Y. (2018). Gypsum, bassanite, and anhydrite at Gale crater, Mars. *American Mineralogist*, *103*(7), 1011–1020. https://doi.org/10.2138/am-2018-6346